2018

The Effect of Cognitive Limb Embodiment on Vascular Physiological Response

Hala Elsir mustafa Osman
Cleveland State University

THE EFFECT OF COGNITIVE LIMB EMBODIMENT ON VASCULAR PHYSIOLOGICAL RESPONSE

HALA ELSIR MUSTAFA OSMAN

Master of Technology
Kent State University
December 2011

Submitted in partial fulfillment of requirements for the degree

MASTER OF SCIENCE IN BIOMEDICAL ENGINEERING

at the

CLEVELAND STATE UNIVERSITY

May 2018

We hereby approve this thesis

For

HALA ELSIR MUSTAFA OSMAN

Candidate for Master of Science in Biomedical Engineering degree for the

Department of Chemical and Biomedical Engineering

and CLEVELAND STATE UNIVERSITY's

College of Graduate Studies

Dr. Paul D. Marasco

Thesis Chairperson

Department of Chemical and Biomedical Engineering

Dr. Antonie van den Bogert

Thesis Committee Member

Department of Mechanical Engineering

Dr. Jeffrey Dean

Thesis Committee Member

Department of Biological, Geological, and Environmental Sciences

Student's Date of Defense: February 12, 2018

DEDICATION

To my precious daughters, Rana and Lana –

You are my inspiration to achieve greatness…

ACKNOWLEDGMENTS

First and foremost, I would like to thank my research advisor Dr. Marasco for guiding me in this challenging research project. His support and knowledge made it possible for me to present this work. I learned so much from him both professionally and personally.

I would like to express my heartfelt thanks to my academic advisor Dr. van den Bogert, who has helped and supported me tremendously. He has cultivated an appreciation for teaching and mentoring students by his example. I would like to gratefully and sincerely acknowledge his mentorship during my graduate education.

I would like to thank Dr. Dean deeply, who has helped and supported me enormously. It will not be an understatement to say that this thesis was enhanced by his guidance. Also, I acknowledge Dr. Fedewa and Dr. Plow from Cleveland Clinic's Department of Biomedical Engineering for their time and effort.

I would like to express my deepest appreciation to my lab members and friends for their limitless support. I would like to thank everyone in the Biomedical Engineering Program at Cleveland State University and Cleveland Clinic who has provided me with their endless support and professional help over the years.

I cannot begin to express my gratitude to my family for all of the love, encouragement, and prayers they have sent my way along this journey. To my parents, thank you for being my champions throughout the past years. Your continuing support has meant the world to me; I hope that I have made you proud.

Last but not least, I want to express my deepest love to my dear husband Salah Garelnabi for his countless sacrifices, constant encouragement, and being there for me all the time. Your support is what has gotten me through when I wanted to give up.

THE EFFECT OF COGNITIVE LIMB EMBODIMENT
ON VASCULAR PHYSIOLOGICAL RESPONSE

HALA ELSIR MUSTAFA OSMAN

ABSTRACT

The rubber hand illusion (RHI) is a visual-tactile perceptual illusion commonly used to study body ownership. In this paradigm, a rubber hand is positioned in front of a participant, and the person's real hand is hidden from sight behind a barrier. When the real hand and the rubber hand are stroked synchronously, individuals perceive the rubber hand as if it were their own; it becomes "embodied." This illusory experience of body ownership is associated with multimodal integration of touch and vision. From these visual-tactile-cognitive mechanisms, we establish that our hands belong to us when what we *see* matches what we *feel*. Recently, studies have established a correlation between the induction of the RHI and temperature changes at the skin surface. Interestingly, when the brain perceives its real limb to be "disembodied" during the cognitive illusion, the temperature of that real limb drops.

The central hypothesis for the proposed study is that cognitive limb embodiment directly affects blood flow patterns; blood flow in a specific limb can be disrupted by altering the sense of the limb's embodiment. Our rationale is that understanding the mechanisms underlying thermal-vascular regulation in healthy and diseased populations is clinically significant because blood flow can be used as a physiological marker of cognitive limb embodiment and may also be particularly important in identifying and understanding disease states.

Physiological correlates of embodiment, such as temperature and blood flow changes, may have significant potential for quantitatively assessing various diseases. The first aim was to develop a modified ultrasound method to measure blood flow under the conditions of the RHI. In addition, the Doppler waveform indices were examined as physiological markers for cognitive embodiment. The second aim was to investigate the link between temperature changes and blood flow during cognitive limb embodiment. Taken together, this work seeks to provide a comprehensive understanding of the effects of cognitive limb embodiment on vascular physiological response.

TABLE OF CONTENTS

Page

LIST OF TABLES

LIST OF FIGURES

NOMENCLATURE

Arteriovenous Anastomoses	AVA
Autonomic Nervous System	ANS
Beats Per Minute	BPM
Baseline	BL
Continuous Wave Doppler	CWD
Doppler Blood Flow	DBF
Doppler Vascular Conductance	DVC
Doppler Vascular Resistance	DVR
End Diastolic	ED
Heart Rate	HR
Laser Doppler Flowmetry	LDF
Mean Arterial Pressure	MAP
Mean Velocity	Vm
Near-Infrared Spectroscopy	NIRS
Oxygenated Hemoglobin	OHB
Parasympathetic Nervous System	PNS
Peak Systolic	PS
Pulsatility Index	PI
Pulsed Wave	PW

Pulsed Wave Doppler	PWD
Resistive Index	RI
Rubber Hand Illusion	RHI
Sympathetic Nervous System	SNS
Total Hemoglobin	THB
Visual Tactile Stimulation	VTS

CHAPTER I

INTRODUCTION

1.1 Motivation

Embodiment can be defined as the perception that our body (or parts of our body) belong to us (Longo et al., 2008). It has been established that bodily experience is a multifaceted process that requires the integration of multiple sensory inputs (Giummarra et al., 2008), and this line of investigation has been closely tied to vision, touch, and proprioception (the sense of where our body is in space) (Tsakiris, 2010). However, the contributions of touch and vision have been the most extensively investigated. This visual and tactile sensory integration has been studied widely through a perceptual phenomenon called the rubber hand illusion (RHI).

In the RHI paradigm, a rubber hand is positioned in front of a participant, and the person's real hand is hidden from sight behind a barrier (Botvinick and Cohen, 1998). When the real hand and the rubber hand are stroked synchronously, participants perceive the rubber hand as belonging to their body; at this point, the actual hand becomes "disembodied" and the rubber hand becomes "embodied." Hence, embodiment can be defined as the state when what the individuals see matches what they feel.

Through the cognitive mechanism of visual-tactile integration, the brain can derive body representation and determine that the rubber hand belongs to the participant (Ratcliffe and Newport, 2017). Interestingly, studies have also suggested that people undergo a physiological response during the RHI. A correlation between the induction of the RHI and skin surface temperature changes has been revealed; when a limb becomes disembodied during the RHI, the temperature of that limb drops (Moseley et al., 2008; Marasco et al., 2011).

Blood perfusion is a primary component of the body's thermoregulatory system. In other words, skin blood vessels dilate in direct response to heat and constrict in direct response to cold. Thus, to maintain blood flow and regulate body temperature, skin perfusion must be responsive to temperature differences (Colberg et al., 2005). Despite the fact that numerous studies have been conducted to investigate the RHI and changes in skin surface temperature, the link between skin surface temperature and blood flow while a person is under the effects of the RHI has not been established**.**

Each blood vessel has its own blood flow pattern which indicates the anatomical and physiological needs of the organ supplied by the vessel (Pries et al., 2005). Thus, blood flow pattern reflects the vessels' status in normal and disease conditions. Therefore, investigating blood flow at a specific vessel under the effect of various stimuli is imperative because flow could be used as a physiological measure of embodiment/disembodiment.

Newer imaging techniques (e.g., thermography, ultrasonography, laser Doppler flowmetry [LDF], and near-infrared spectroscopy [NIRS]) are all being adapted to measurements of blood flow.

1.2 Specific Aims

Ongoing research is moving towards a better understanding of the mechanisms of regulating skin blood flow, as these mechanisms are often damaged in many diseases. The central hypothesis is that blood flow in a specific limb can be altered by disrupting the sense of embodiment. The rationale for this research is that understanding the mechanisms underlying thermal-vascular regulation in healthy populations is clinically significant because estimation of the temperature-blood flow association can provide useful information for the diagnosis of various diseases. The link between blood flow and skin surface temperature changes during cognitive embodiment has not yet been established.

The first aim of this study was to quantify the relative change in volume flow during the RHI. To do this, a modified Doppler ultrasound method was developed. Then, the estimated Doppler blood flow was measured by using the modified method under the effect of the RHI. In addition, two Doppler waveform indices – pulsatility index (PI) and resistive index (RI) – were examined for potential use as physiological measures of cognitive embodiment.

The second aim of this study was to investigate the link between temperature and blood flow changes during the RHI by using three physiological measures: (1) a physiological infrared thermal imaging system to capture variations in skin temperature in the hand; (2) near-infrared spectroscopy (NIRS) to measure tissue blood flow in the forearm; and (3) laser Doppler flowmetry (LDF) to measure the skin blood flow in the hand. The objectives of the studies done for this thesis are twofold, as shown in Figure 1.

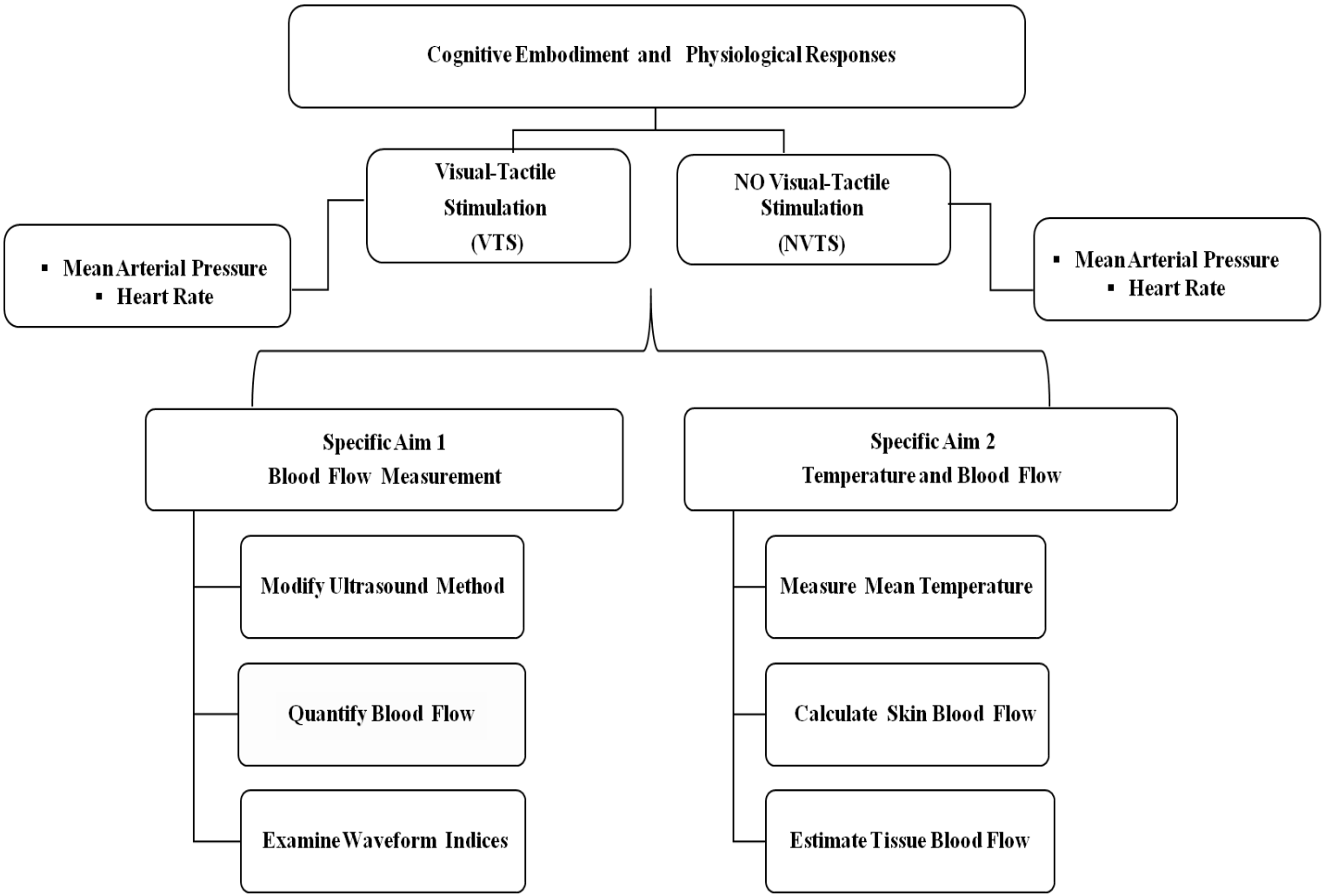

Figure 1: Overall Goal

1.3 Significance of Research

The key contribution of our first study is that using the noninvasive modified ultrasound method provides a means of linking volumetric flow quantification to thermal changes that occur under the cognitive embodiment. Doppler waveform indices such as PI and RI reflect important physiological information that can be used as tools in the clinical evaluation of disease. These indices have particular advantages over the blood-flow-velocity measurement, as the need for the Doppler angle correction and the vessel diameter measurement was nullified when these indices were calculated in the ultrasound system. This is a significant advantage, particularly when imaging small vessels. Another advantage is that these indices depend on the peak-systolic, end-diastolic, and mean velocities, which provide more sensitivity in making a distinction between different types of waveforms.

One of the primary benefits of our second study is the clinical importance of investigating the link between vascular and thermal changes, as it provides insights into the mechanisms of the RHI's physiological correlates. Another advance is the algorithm we have developed to read the data images and compute the mean temperature on both the experimental and control hand simultaneously.

Capturing variations in the limb's mean skin temperature, in the whole hand from wrist down to fingertips, confers a significant advantage as it minimizes sources of error. Hence, in comparison with other techniques, this method has the advantage of continuous measurement throughout the experiment to ensure accuracy and reliability of the results.

1.4 Scope of Thesis

This thesis is organized into five chapters. Chapter 1 presents the motivation of this work, as well as the significance and contribution to the field. Chapter 2 presents a literature review, describing RHI induction and measures. It also highlights the importance of quantitative assessment of vascular blood flow, provides an overview of the circulatory system, and illustrates some typical clinical techniques used for monitoring flow: Doppler ultrasound, LDF, and NIRS. In it, we address temperature regulation and control as well. Chapter 3 explains study 1; its purpose was to quantify the relative changes in blood flow and provide detailed information about how the modified Doppler ultrasound method was used to measure blood flow. In addition, the Doppler waveform indices were explored for use as physiological markers of cognitive embodiment. Chapter 4 describes study 2; its aim was to investigate the link between skin surface temperature and peripheral blood flow. Chapter 5 summarizes the conclusion of this work and offers some future directions by which to continue investigating this line of research.

CHAPTER II

BACKGROUND AND LITERATURE REVIEW

2.1 Cognitive Limb Embodiment

2.1.1 Induction of the RHI

To induce the RHI, a rubber hand was positioned in front of the subject within an appropriate visual reference frame, while one of their actual hands was hidden behind a wooden barrier. Two paintbrushes were used to induce the illusion by stroking both the rubber hand and the participant's real hand synchronously.

One should therefore be aware of the differences between the manual and automated stroking, as it plays an important role in evoking the RHI effect. Some researchers have used manual stroking to induce the RHI (Botvinick and Cohen, 1998; Moseley et al., 2008; Marasco et al., 2011; Rohde et al., 2013), while others have used automated stroking to elicit the illusory experience (Rohde et al., 2013). These two experimental setups differ for example in the presence of the experimenter (in the case of manual strokes) and in pressure of stimulation (person versus machine). Individuals have shown a stronger RHI response when manual strokes were used (Rohde et al., 2013).

Subjects were instructed to look at the rubber hand while the experimenter induced the illusion by stroking both the participants' hand and the rubber hand at the same time in the same way. At the end of each trial, subjects were asked to fill out a questionnaire and to state whether they agreed or disagreed with the statements and assign values on a 7-point scale ranging from 'strongly agree' (+3) to 'strongly disagree' (-3). Higher numerical values on these statements indicate a more vivid illusory experience. The self-report questionnaire is adapted from the original work done by Botvinick and Cohen in 1998. The questionnaire consists of two parts (Table 1).

Table 1: Statements Listed on the Participant Questionnaire.

Illusion Statements:

1. It seemed as if I were feeling the touch of the paintbrush in the location where I saw the rubber hand located.
2. It seemed as though the touch I felt was caused by the paintbrush touching the rubber hand.
3. I felt as if the rubber were my hand.

Control Statements:

4 It felt as if my (real) hand were drifting towards the right (towards the rubber hand).
5 It seemed as if I might have more than left hand or arm.
6 It seemed as if the touch I was feeling came from somewhere between my own hand and the rubber.
7 It felt as if my (real) hand were turning 'rubbery'.
8 It appeared (visually) as if the rubber hand were drifting towards the left (towards my hand).
9 The rubber hand begun to resemble my own (real) hand, in terms of shape, skin, freckles or some other visual feature.

The first part has three statements (Q1-Q3) that reflect the participant's cognitive limb embodiment experience: (Q1) 'It seemed as if I were feeling the touch of the paintbrush in the location where I saw the rubber hand'; (Q2) 'It seemed as though the touch I felt was caused by the paintbrush touching the rubber hand'; and (Q3) 'I felt as if the rubber hand were my hand.'

The magnitude of agreement with the statements indicates the strength of the illusion. The second part contains 6 statements (Q4-Q9) that were used as control statements. The statement questions were presented in a randomized order to ensure proper outcome. A key point to mention here is that, in order for embodiment to take place, two fundamental conditions must be met: first, the rubber hand and the participant's real hand have to be stroked synchronously; and second, the rubber hand should be positioned within an anatomically and visually reasonable location. This means that the experience of embodiment depends on multiple sensory integration (Ehrsson, 2005; Lane et al., 2017). In other words, when what the individuals see matches what they feel, embodiment happens; at that point, the actual hand becomes disembodied and the rubber hand becomes embodied.

2.1.2 Measurements of the RHI

Typically, self-report questionnaires of the subjective illusory experience and proprioceptive drift distance are the most commonly used measures used for the RHI. The experience of the RHI has often been measured explicitly through psychophysical questionnaires to gauge the vividness of the illusion. Although questionnaires offer a quantifiable measure of participants' experience in relation to the illusion, this method has its limitations, since it involves inter-individual variability of subjective illusory experience (Valenzuela Moguillansky et al., 2013).

The knowledge of where our body is in space is defined as proprioception. The difference between where the participant's real hand is located and where the participant perceives the hands to be after experiencing the RHI is known as proprioceptive drift.

Several studies have demonstrated that proprioceptive drift is consistent with the reported illusory experience, indicating that it is a valid measure of the illusion. Yet other studies found proprioceptive drift to be an unreliable measure (Kammers et al., 2009; Rohde et al., 2011; Lane et al., 2017). Therefore, more objective and dependable measures to investigate the effects of the RHI are needed. Implicit measures have been used to quantify the physiological correlates of the RHI, such as skin surface temperature.

2.1.3 Laterality and Hand Dominance of the RHI

A number of studies have established that handedness does not affect the vividness of the RHI (Ocklenburg et al., 2011; Smit et al., 2017). The experience of the RHI for the left and right hand in healthy populations is the same because both hands may have similar representation in the brain (Ocklenburg et al., 2011). Vessel diameter differs between both limbs, and it is significantly larger in the dominant limb (Kagaya et al., 2010). Thus, in this study more attention was given to the dominant limb.

2.2 Temperature and Blood Flow

Blood flow measurement offers critical information for the diagnosis of various diseases (Calamante et al., 1999). The disruption of flow outside the typical range can pose serious consequences for local tissue, and therefore it can be used as an indicator of a number of diseases, including heart disease, stroke, hypertension, and diabetes. Recent advances in medical imaging provide more comprehensive techniques for blood flow evaluation in various diseases. Several studies have established that individuals with diabetes have a greater risk of vascular disease (de Galan et al., 2009).

Using thermal imaging as a noninvasive technique can yield valuable information regarding the physiological processes in the course of skin surface temperature, distribution, and blood perfusion (Sivanandam et al., 2012). A digital infrared thermal imaging system used for medical purposes (Meditherm, Cheyenne, WY) is designed to monitor thermal abnormalities occurring in numerous diseases, as it allows the examiner to visualize and quantify changes in skin surface temperature (Bagavathiappan et al., 2010; Sivanandam et al., 2012). Thermal imaging is commonly used in the early detection of diabetes (van Netten et al., 2013). Since there is a great degree of thermal symmetry in the normal limb, subtle abnormal temperature asymmetries can be easily identified.

Skin surface temperature is mainly regulated through peripheral vasoconstriction and vasodilation mechanisms. Although the brain controls the regulation of body temperature, the skin plays a major function in conserving or dissipating heat. For instance, the brain triggers constriction of the blood vessels within the skin when body temperature begins to drop below normal, which in return decreases heat loss from the skin surface (Berne et al., 2008). In the healthy population, there is a symmetrical dermal pattern across the body, which is consistent and reproducible for any individual (Holowatz and Kenney, 2010); thus, any noticeable difference in skin temperature can be identified.

2.3 The Circulatory System

2.3.1 General Description

The circulatory system consists of three independent systems that work together: the heart, blood vessels, and the blood itself. There are three major types of blood vessels: arteries, capillaries and veins. The main function of the circulatory system is to transport nutrients and oxygen, to remove metabolic waste products (carbon dioxide and nitrogenous wastes), and to regulate blood pressure and body temperature. Early manifestations of diseases may be encountered in the microcirculation (Berne et al., 2008).

This maladjustment can occur due to either damage to the microcirculation or to the blood itself. The microcirculation is responsible for the distribution of blood within tissues, and it describes the blood flow throughout the microvasculature that comprises arterioles, capillaries, and venules.

2.3.2 Why Choose the Brachial Artery?

For the purpose of this study, we planned to focus on the brachial artery (and its extensions into the hand) for several reasons. Although arteries and veins both carry blood around the body, they differ; systemic arteries carry oxygenated blood from the heart to the rest of the body, whereas systemic veins carry deoxygenated blood from the rest of the body back to the heart.

In normal arteries, flow velocity increases rapidly to a peak during early systole and decreases during diastole, when flow reversal can occur. The brachial artery (Figure 2), a major blood vessel located in the upper arm, is the main supplier of blood to the arm and hand. Arterial walls are thick, while the lumen is small in diameter.

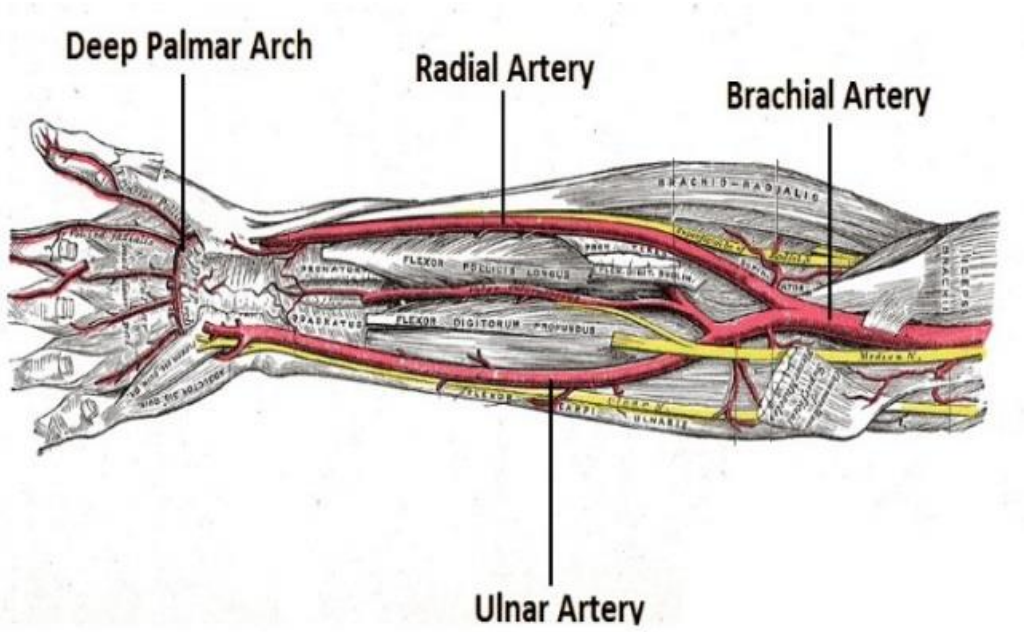

Figure 2: Illustration of Upper-Limb Arteries in Right Hand (Jones, 2017).

Arteries are elastic and are adapted for carrying nutrients and blood away from the heart under considerable pressure that is needed to maintain blood flowing rapidly to the rest of body. Therefore, to obtain optimal results from our RHI research, we chose to measure changes in blood velocity in the brachial artery.

2.3.3 Heart Rate and Blood Pressure Regulation

From the literature, it is known that the autonomic nervous system (ANS) is responsible for controlling blood pressure, including contraction of the heart, peripheral resistance of blood vessels, and the heart rate. Two major branches of the ANS work together: the sympathetic nervous system (SNS) and the parasympathetic nervous system (PNS). One can define blood pressure as the force the blood exerts against the walls of arteries. Systolic pressure (the pressure at the peak of ventricular contraction) is the pressure as the heart beats and forces blood into the arteries; diastolic pressure occurs

when ventricles relax, and it is a measure of the pressure as the heart relaxes between beats (Berne et al., 2008). A normal blood pressure reading is 120/80 mm Hg. The normal heart rate is defined as the number of heart beats per minute (bpm).

Heart rate (HR) and mean arterial pressure (MAP) are controlled by both SNS and PNS. Blood pressure and vessel diameter are inversely related. In other words, during increasing vessel vasodilation, arterial pressure is reduced, and arterial pressure is increased during decreasing vessel vasoconstriction (Berne et al., 2008).

2.4 Ultrasound Imaging

For a two-dimensional imaging system such as ultrasound, spatial resolution comprises axial and lateral components (Figure 3). Axial resolution provides useful information that specifies the imaging system's capability to measure tiny features precisely. A key point is that while having a greater axial resolution is a positive feature, there is a trade-off with imaging depth; the shorter the wavelength, the higher the spatial resolution and the higher the imaging frequencies, but lesser penetration. Thus, a relatively lower-frequency linear transducer is used to ensure a better penetration to image deeper structures in the brachial artery. In contrast, the ultrasound pulse attenuates more quickly as frequency increases, which then limits imaging depth (Maulik, 2005).

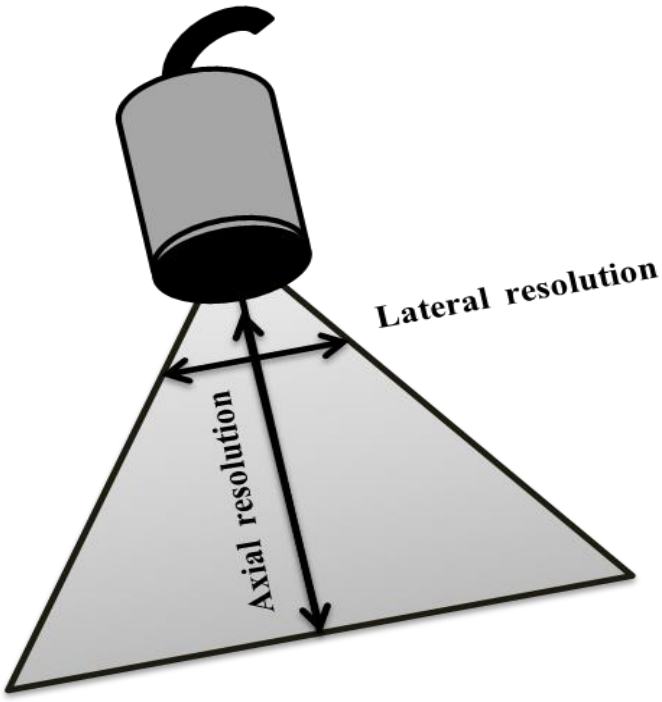

Figure 3: Different Ultrasonic Beam Resolution.

In other words, the speed at which the returning echo reaches at the transducer is proportional to the depth of the scattering boundary.

2.4.1 Pulsed Wave Doppler

Pulsed-wave (PW) Doppler sonography uses the Doppler principle that moving objects change the characteristics of the sound waves generated. The PW technique employs piezoelectric ceramic elements of the transducer that emit and receive ultrasonic waves in pulses. It is established that piezoelectric materials are designed to generate and detect sound waves (Maulik, 2005). The same transducer is used for transmission and reception of these ultrasonic signals. The number of pulses per second is known as the pulse repetition frequency; this factor depends on depth and velocity (Maulik, 2005).

That is because the system calculates the time between transmitting and receiving the signals (time-of-flight) corresponding to a specific position and location on the vessel (Figure 4).

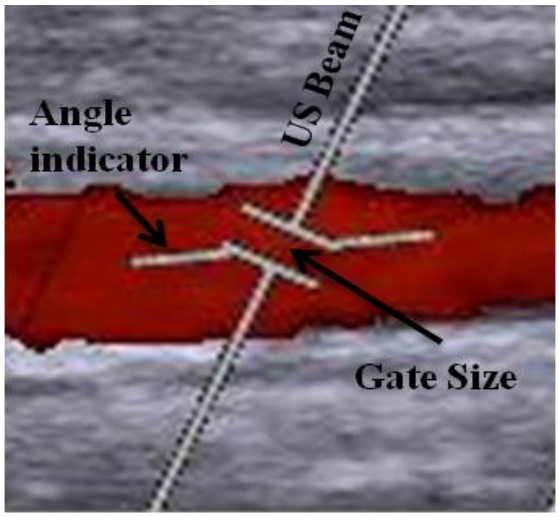

Figure 4: Pulsed Wave Doppler.

Therefore, the flow measurement information is determined based on the size and location of the Doppler gate size in the longitudinal direction (axial resolution).

2.4.2 Doppler Waveform Indices

The Doppler spectrum is defined as a time-velocity waveform that represents variation in blood-flow velocities during the cardiac cycle, as shown in Figure 5. These velocity distributions serve as diagnostic parameters in evaluating blood flow and pathophysiology (Nelson and Pretorius, 1988). The Doppler spectrum is used to reflect the physiological condition of the organ that is supplied by the vessel.

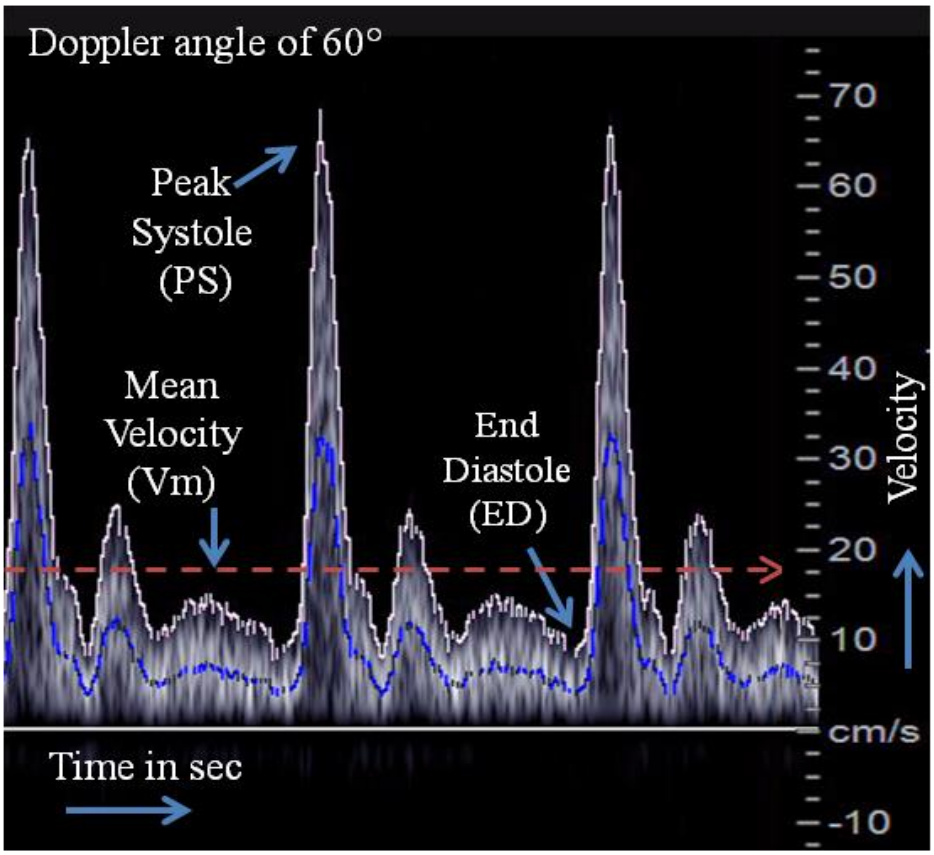

Figure 5: Display of Doppler Spectrum.

Doppler waveform analysis is frequently used as a diagnostic tool in the clinical assessment of disease and can be expressed by relatively simple waveform indices. The commonly used waveform indices are the PI and RI. The PI can be defined as the measure of variability of blood velocities within the vessel (Petersen et al., 1997), equal to the difference between the peak systolic (PS) and minimum diastolic (ED) velocities divided by the mean velocity (Vm) during the cardiac cycle (Eq. 1).

$$Pusatility\ Index\ (PI) = \frac{PS - ED}{Vm} \quad (1)$$

The RI, developed by Léandre Pourcelot, can be defined as a measure of pulsatile blood flow that reflects the resistance to blood flow caused by the microvascular bed distal to the site of measurement (Eq. 2).

$$Resistive\ Index\ (RI) = \frac{PS - ED}{ED} \quad (2)$$

The RI has been used as a marker of renal function and pathology in kidney disease (Sung et al., 2017), where the normal RI range is 0.50-0.70; any higher or lower value may point to a disease state (Hanamura et al., 2012). Additionally, the RI and PI are reliable for evaluating peripheral vascular disease (Lin and Spratt, 1997); these two indices also provide information about blood flow and vascular resistance that is difficult to obtain from the velocity measurement alone (Chavhan et al., 2008).

Differences in peak systole and peak diastole frequently reflect important physiological information that can be represented by the waveform indices RI and PI. Hence, within the context of the RHI, the RI and PI can potentially be used as diagnostic tools to reflect physiological responses under the effect of external stimuli.

2.5 What Remains Unknown?

Many questions remain unanswered in regard to the perceptual illusion and physiological changes related to characteristics of blood flow measurement. For example, “How can we best estimate blood flow under the effect of the illusion?” The answer to this question involves the use of PW Doppler ultrasound and can be applied to measure blood flow responses under different conditions. Additionally, the obtained information can be used to explore Doppler waveform indices as physiological markers of the sense

of embodiment. Other unanswered questions are “How are blood perfusion and skin surface temperature related during the cognitive limb embodiment? What is the connection between the temperature and blood flow changes during the RHI?” Gaining an understanding of these concepts will offer insights into the mechanisms of the RHI’s physiological correlates. Here, we can examine the effects of peripheral vasoconstriction on blood pressure and HR, and how these are related to vessel diameter. Clinically, this information will allow us to recognize the crucial role of peripheral resistance in influencing local blood flow. The questions presented can be answered through an investigation into the effect of cognitive limb embodiment on vascular physiological response.

CHAPTER III

QUANTIFICATION OF ESTIMATED DOPPLER BLOOD FLOW

3.1 Introduction

Doppler ultrasonography is an accurate, noninvasive method for investigating volume flow and diagnosing a range of diseases that influence blood flow (Sung et al., 2017). It is a technique that provides critical information on underlying physiological processes in healthy and diseased populations. The central research goals of Doppler ultrasonography are to offer accurate and reliable measurement of blood flow through the arteries (Evans, 1985; Casey et al., 2008).

Several studies have established that measurement of the cross-sectional area of a vessel is critical to volume flow estimation when using the Doppler ultrasound technique (Li et al., 1993; Kagaya et al., 2010). In both vascular research and pharmacologic studies, measurement of blood vessel diameter is a standard technique by which to compare vasoconstriction before and after treatment (Fischer et al., 2010). Blood vessels can change structure in response to various conditions to meet functional demands (Nelson and Pretorius, 1988).

Tracking changes in vessel diameter is a time-dependent process that requires high accuracy of measurements (Hiltawsky et al., 2003). Variations in arterial diameters throughout the cardiac cycle (Evans, 1985) make it challenging to estimate blood flow and may introduce errors. Many studies have documented errors associated with blood flow estimation using ultrasound (Gill, 1985; Hoskins, 1990; Zierler et al., 1992). Errors in measurement of volume flow from an ultrasound system result from errors in velocity and area determination (Zierler et al., 1992). These recognized inaccuracies have encouraged study into modified measurement techniques to reduce these sources of error (Berg et al., 2000; Rubin et al., 2001; Hoyt et al., 2009).

Since the use of an ultrasound system to achieve accurate quantitative blood flow measurements is exceedingly beneficial for clinicians and researchers, substantial effort to reduce these sources of error are still needed (Hoyt et al., 2009). There is an unmet need for an accurate and reliable approach to obtaining quantitative blood flow measurements.

To measure blood flow velocity within the blood vessel, ultrasound waves are transmitted into a vessel and the sounds reflected from the blood are detected. The velocity is determined from the Doppler shift frequency. A frequency shift (Doppler shift) is described in Eq. 3:

$$Fd = Fr - F0 = \frac{2 * F0 * Vm * \cos\theta}{c} \tag{3}$$

where *F0* is the transmitted frequency, *Fr* is the received frequency, *Fd* is the Doppler shift, *Vm* is the flow velocity, *c* is the speed of sound, and *theta* (θ) is the Doppler angle. The original frequency is multiplied by 2 since the Doppler shift occurs twice: when the

transmitted wave is incident on the moving red blood cell and when the moving red blood cell reflects it back. Local blood flow is affected by changes in arteriolar constriction; the smooth muscle contracts, leading to a decrease in the vessel diameter. Three main factors determine the resistance to flow.

According to Poiseuille's equation $\boldsymbol{R = \eta L / r^4}$, vessel resistance (R) is directly proportional to the length (L) of the vessel and the viscosity (η) of the blood, and inversely proportional to the radius to the fourth power (Berne et al., 2008). A small change in vessel diameter leads to a large change in resistance. For instance, if the vessel is decreased by half, blood flow is reduced by factor of 16. One study established that changes in arterial resistance occur from alterations in blood-vessel diameter (Hoskins et al., 2017).

To measure blood flow in a given region, vessel diameter is calculated. It is commonly established by researchers that blood vessels have a circular cross-sectional area ($A = \pi r^2$), where r equals the radius. Thus a measure of blood flow can be calculated from a measure of the radius (Eq. 4).

$$Blood\ \ Flow(ml/min) = Mean\ Velocity(cm/sec) * Area(cm^2) * 60 \quad (4)$$

Typically, blood-flow calculations involve measuring the mean velocity (Vm) of flowing blood within a vessel, multiplying that mean by the cross-sectional area of the vessel lumen, then multiplying by 60 to convert to minutes.

3.2 Issues with the Standard Blood Flow Measurement

Even though the standard method of measuring blood flow has been used by numerous researchers in several disciplines, we determined that it was not appropriate for our study for several reasons. Using Doppler ultrasound to determine volume flow in a region requires the Doppler gate to be exactly placed to encompass the whole blood vessel. However, this is not possible (Evans, 1985), particularly for the purpose of this study, which is to quantify the relative changes in volume flow in the brachial artery (longitudinal direction) under the effects of the RHI.

One of the major concerns about using the standard method for our study was the technical difficulty in keeping the ultrasound transducer in a position to encompass the vessel diameter throughout the experiment to allow us to detect blood flow under the effect of the illusion. Additionally, it is nearly impossible to eliminate the slight but unavoidable arm-shifts while still maintaining throughout the entire experiment more accurate and reliable measurements on the exact region being examined. As soon as movement occurs, data will be inaccurately recorded or lost.

In our earlier preliminary studies, collecting flow velocities for even a few minutes was impractical and induced fatigue. Moreover, correct estimation of the angle between the ultrasound beam and blood flow direction is problematic, and any errors can be magnified. For all the mentioned issues, the standard method is inappropriate and does not support the main goal of this study, which is to investigate the connection between the RHI and actual vascular changes. This situation highlights the need for a modified method to determine volume flow under the conditions of the illusion. Therefore, in this

first study, there were three sub-aims: **(1)** develop a modified method that both considers the induction of the RHI and the ultrasound system for measuring blood flow accurately; **(2)** quantify the relative change in volume flow in the given region per unit time; and **(3)** examine the hypothesis that waveform indices such as the RI and PI can be used to link these waveform indices to physiological quantities such as vascular resistance.

3.3 Measuring Blood Flow during the RHI: A Modified Approach

Our modified ultrasound method focuses on the three major aspects that affect blood-flow measurement when using Doppler ultrasound: **(1)** Doppler gate **(DG), (2)** Doppler angle **(Θ)**, and **(3)** Doppler vertical length (**DL)**, as illustrated in Figure 6.

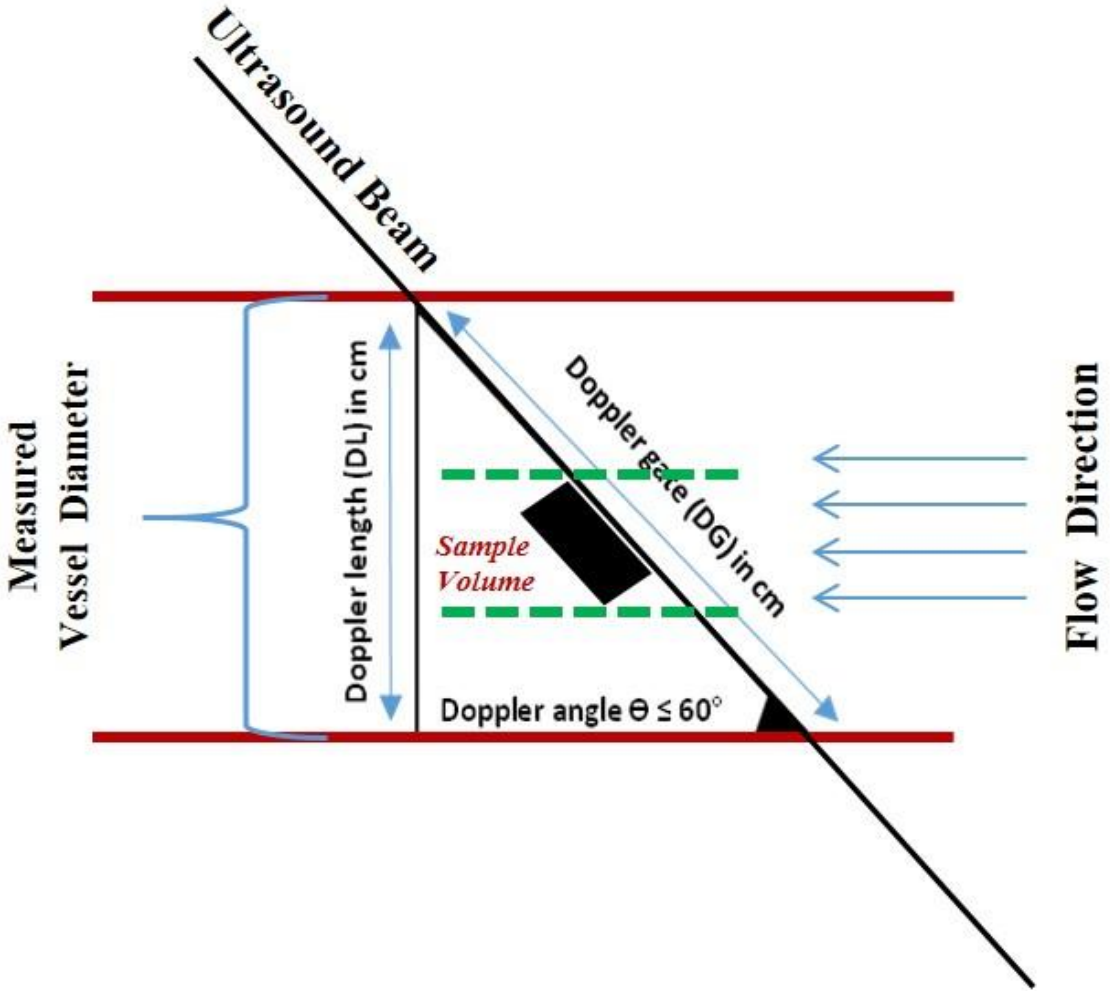

Figure 6: The Standard Method for Blood Flow Measurement.

3.3.1 Doppler Gate

The size of the DG is a significant factor, as it determines sampling volume within the blood. The range of the DG size is principally governed by the size of the blood vessel itself; for instance, a larger vessel needs a larger DG size to encompass the entire vessel diameter. The location of the DG plays an important role, as it influences which velocity of flow contributes to the Doppler signal. In laminar flow, the blood velocity in the vessel's center is greater and slowest near the vessel wall. Thus, placing the DG in the center provides velocity measurements that are more consistent and less sensitive to position change.

It has been established that on average the brachial artery diameter equals 5 mm (Chami et al., 2009). Based on various studies, it has been reported that a waveform typically is seen in vessels with a diameter of <5 mm (Chavhan et al., 2008; Chami et al., 2009). Additionally, from our initial developmental trials, we learned that the DG should be placed in the center of the vessel. It has been established that arterial diameter varies throughout the cardiac cycle (Evans, 1985), so these variations may alter the type of flow and thus the associated velocity distributions (e.g., laminar, turbulent, flat), so a change in DG size affects the blood flow, waveform, and velocity distribution measurements (Nelson and Pretorius, 1988).

Using different gate sizes is unsuitable when the focus of the study is to determine the effects of an external stimulus on blood flow and velocity measurements. Therefore, a DG size of 1.3 mm was used in all the flow measurements for these reasons: **(1)** keep the gate within the vessel despite participant movement; **(2)** avoid wall noise; and **(3)** eliminate signals from neighboring vessels.

3.3.2 Doppler Angle

The angle correction of beam insonation is a very significant process by which the Doppler angle (θ) is estimated, as it involves aligning the angle indicator on an ultrasound image along the longitudinal axis of the blood vessel. The cosine of this angle is used in the Doppler equation (Eq. 3) for calculating velocity from Doppler shift frequency. When cosine θ equals 1, the ultrasound beam is parallel to the blood flow direction, and when cosine θ equals 0, the beam is perpendicular to the blood flow direction (no Doppler shift).

The amount of the error depends on the angle used (Nelson and Pretorius, 1988; Zierler et al., 1992). In other words, a small Doppler angle causes a small error, whereas a large Doppler angle results in a great error. It is known that there is a link between error and angle variability; greater variability in velocity calculations occurred when different Doppler angles were used (Blanco, 2015). Thus, common clinical practice is to use a Doppler angle of 60° or less to minimize the error in angle correction. However, from our bench-test trials, we have learned that it is difficult to use a Doppler angle smaller than 60° while retaining continuous velocity measures at the selected area of the brachial artery throughout the testing time. Therefore, to decrease the magnitude of error and variability of using different Doppler angles for each participant, we concluded that the Doppler angle should be set to a constant value of 60°.

The intention here was to set the ultrasound transducer to align at a Doppler angle of 60° for all velocity measurements across all participants for consistency purposes to ensure the intra- and inter-individual repeatability of the approach.

3.3.3 Doppler Vertical Length

It should be noted that the DG was located inside the vessel lumen rather than covering the whole vessel diameter, therefore we needed to find a substitute vessel diameter, as shown by the dotted line and noted '*calculated vessel diameter'* in Figure 7. This decision was based on the Pythagorean theorem equation $\mathbf{a^2 + b^2 = c^2}$, in which **a** represents the Doppler vertical length (DL) and **c** represents the fixed DG size.

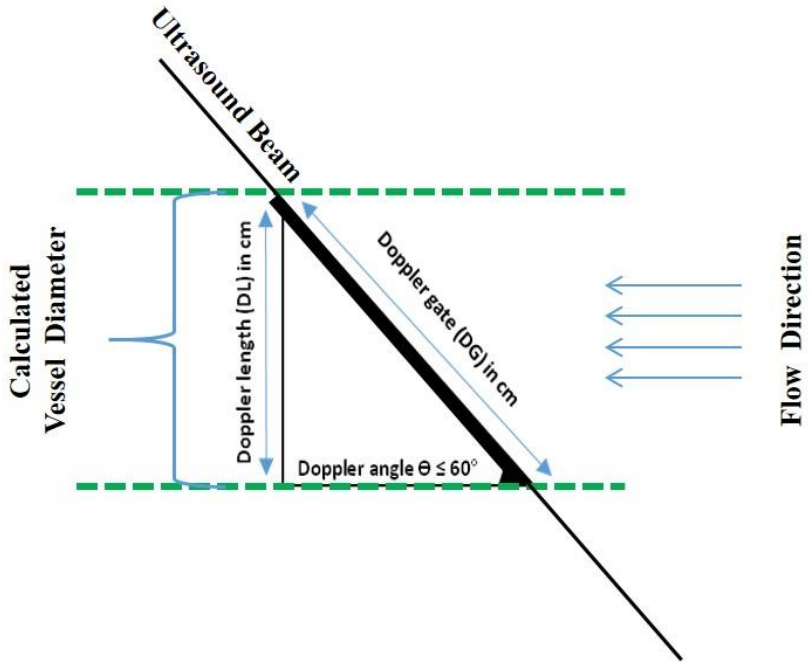

Figure 7: Modified Method for Blood Flow Measurements Under the RHI.

Since the Doppler angle (60°) and DG size (1.3 mm) were known, the vertical distance (DL) can be calculated, as it is equal to the opposite side shown in Eq. 5. To find the DL, we substituted the known value of the DG size (the hypotenuse) into the Pythagorean theorem.

$$opposite\ side\ = sin\ (\theta) * hypotenuse \quad (5)$$

Then, we estimated the circular area $A = \pi r^2$ by using the DL equal to the vessel diameter, as shown in Eq. 6.

$$DL(cm) = \frac{DG(cm) * sin\,\theta}{2} \quad (6)$$

Therefore, the estimated circular area can be calculated as shown in Eq. 7.

$$Area\ (cm^2) = \pi * \left(\frac{DG\ (cm) * sin\,\theta}{2}\right)^2 \quad (7)$$

Then, blood flow was calculated using the new estimated circular area, and that value was substituted in Eq. 2 to produce the modified Doppler blood flow (DBF) equation, shown in Eq. 6, as expressed in milliliters per minute.

$$DBF(ml/min) = Vm\ (cm/sec) * \pi * \left(\frac{DG\ (cm) * sin\,\theta}{2}\right)^2 * 60 \quad (8)$$

MAP was measured using a finger cuff on the third digit of the stimulated hand and expressed in mm Hg. After the DBF measurements were obtained, we then calculated the Doppler vascular conductance (DVC) as expressed in ml/min/mm Hg, as shown in Eq. 9.

$$DVC\ (ml/min/mm\ Hg) = \frac{DBF\ (ml/min)}{MAP(mm\ Hg)} \quad (9)$$

3.4 Potential Limitations

This work provides an exciting opportunity to advance our knowledge with a new experimental application for Doppler ultrasound, as it offers some important insight to better understand the connection between blood flow and the RHI. Some limitations of this modified method may possibly be due to technical and anatomic factors. In the cases where it was difficult to locate the brachial artery with a Doppler angle of 60º to obtain a quality image, the inverse of the Doppler angle (-60º) was used instead.

Since the purpose of this study was to investigate the relative changes in blood flow within the DG size rather than the net blood flow, the retrograde flow was ignored and absolute velocity values were used for determining the DBF measurements. Additionally, this method might have been much more interesting if we had used a second ultrasound system on the subject's control hand to compare the blood flow of both hands simultaneously. On the other hand, finding a twin-system was not possible and using a different system may have introduced variation. This work makes a key contribution to bridging the gap between cognitive limb embodiment and blood flow measurement.

3.5 Methods

3.5.1 Participants

Twelve healthy volunteers (7 male, 5 female; all right-handed [one ambidextrous]; age range, 23-48 years; mean ± SD, 30.3 ± 9.01 years) were recruited (Table 1). Eleven participants successfully completed the experiments; one male participant (Par 6) was excluded due to failure to maintain the transducer in position.

This study was approved by the Institutional Review Board (CCF IRB#14-402). All participants gave their written informed consent prior to participation.

Table 2: Characteristics of Human Subjects.

Participant	Gender	Dominant Hand
1	Male	Right
2	Male	Right
3	Female	Right
4	Female	Right
5	Female	Right & Left
6*	Male	Right
7	Mal	Right
8	Male	Right
9	Male	Right
10	Male	Right
11	Female	Right
12	Female	Right

**Data were excluded from further analysis.*

3.5.2 Experimental Setup

Due to some logistics and setup limitations, multiple modalities were combined in one complex experiment design. The data for Study 1 and Study 2 were collected at the same time in one experimental setting. In **Study 1**, three trials for each hand were performed, and each trial contained 2 periods: Baseline (BL, 2 min) and Visual Tactile Stimulation (VTS, 6 min). In **Study 2**, three trials for each hand were performed, and each trial contained 3 periods: Baseline (BL, 2 min), Visual Tactile Stimulation (VTS, 6 min), and Visual Fixation (VF, 2 min).

Participants' dominant hand (i.e., the right hand) was tested first in all experiments. A multichannel data-acquisition module was used to enable analog voltages from externally connected systems to be captured with Lab Chart software

(ADInstruments, Colorado Springs, CO) for further analysis offline. The data generated from ultrasonography and thermography were collected separately in their own systems.

3.5.3 Experimental Procedure

The experiment was carried out in a quiet room at constant room temperature. Participants were seated in front of a table, with both arms placed on the table. A piece of memory foam was placed under the participant's arms to minimize the effect of table-surface temperature on the participant's skin temperature as well as to provide comfort throughout the testing period (Figure 8).

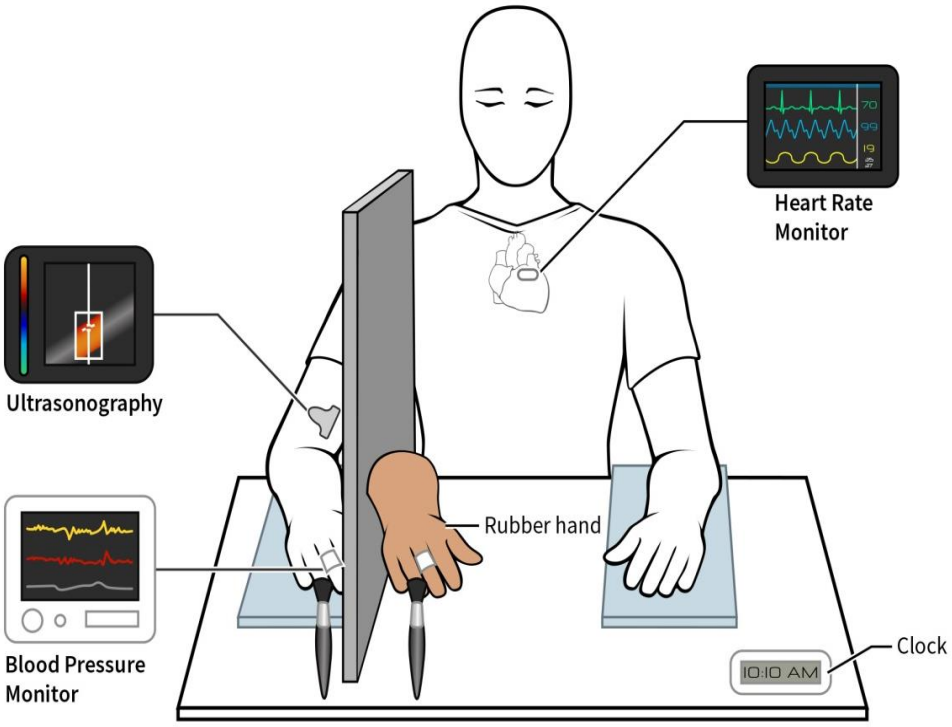

Figure 8: Experimental Setup for Measuring Doppler Blood Flow.

For each participant, three trials for each hand were performed. Each trial contained 2 periods: Baseline (BL, 2 min), Visual Tactile Stimulation (VTS, 6 min). In BL**,** participants were blindfolded and wore earplugs and headphones to block any noise or distraction from the surrounding area. During VTS, participants were asked to sit comfortably.

The RHI was administered twice; a right rubber hand was used to induce the illusion onto the participant's real right hand and a left rubber hand was used to induce the illusion on the participant's real left hand. To avoid fatigue and to ensure proper blood flow to the tested hand, participants were instructed to move and relax their arms after completing their right-hand stimulation trials.

It is well known that synchrony and asynchrony are the two types of stroking conditions that are commonly used to induce the illusion when performing RHI research. It has been reported and generally accepted that the illusion is stronger when using a synchronous than an asynchronous stroke. Therefore, the focus here was to use the synchronous stroking condition to ensure the strongest achievable difference between test and control conditions. Thus, in this work, we also decided to use nonstroking as a control condition instead of asynchronous stroking.

A key point to keep in mind to fully appreciate our study's experimental procedure is that the questionnaires commonly used to equate the strength of the RHI among participants reveal that the subjective experience differs among individuals. Therefore, in this investigation, our center of attention was to use several measures of the hemodynamic parameters, including blood pressure, HR, blood flow velocities, and

vascular conductance to detect changes in the vascular parameters. In addition, the relationships among these parameters are significant to our understanding of the Doppler information obtained in this work.

3.5.4 Ultrasound Measurement

Doppler ultrasound was used only on the right hand. A coupling gel was applied to participants' skin to ensure proper image quality. The transducer 9L4 (2D mode, 4-9 MHz; Doppler, 4-6.75 MHz) was appropriately placed, without compression, on the participant's arm over the brachial artery. The ultrasound transducer was attached onto a customized 3D-printed transducer-shaped holder that was affixed onto the testing table by an armature to maintain the Doppler angle of 60° during the entire testing session. The DG with a sample gate of 1.3 mm was used in all the measurements.

While ultrasound systems can determine blood velocities, several steps were needed during data collection. For instance, images were first stored onto a hard drive of the ultrasound system and then exported into a compatible file format known as Digital Imaging and Communications in Medicine (DICOM) for further image post-processing. Data collection processes were as shown in Figure 9.

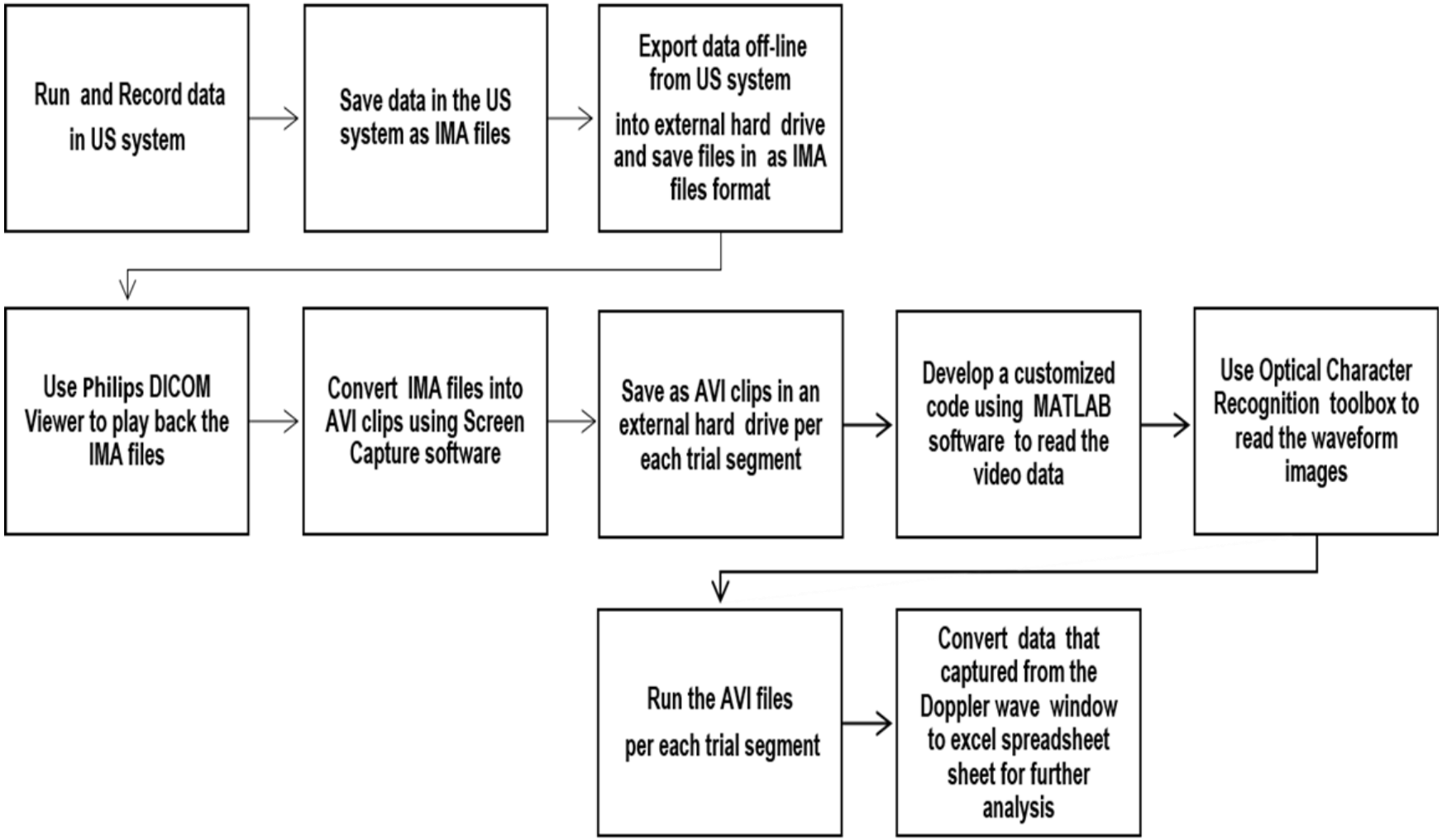

Figure 9: Overview of Different Processes for Doppler Ultrasound Data Collection.

3.5.5 Data Collection

Doppler measurements of Vm, PI, and RI were collected. MAP was measured using a finger cuff on the third digit of the stimulated hand. HR was monitored and used as an internal control. The HR device was calibrated according to each participant's height and weight. DBF was calculated (Eq. 6), and DVC was then calculated as shown in Eq. 7. Since the DVC is equal to the reciprocal of resistance, we then calculated the Doppler vascular resistance.

3.5.6 Statistical Analysis

Statistical analysis was performed using the statistical package Minitab software (Minitab Inc., State College, PA). Comparison between BL and stimulation was conducted using a paired *t* test with a 95% confidence interval (CI) for mean difference. The results presented here are always in terms of comparison between the stimulated hand and the control condition as means ± standard error of the means. A significance level of $\alpha = 0.05$ was used.

3.6 Results

3.6.1 Responses to Questionnaires

The questionnaire responses were used to evaluate the participants' experience when the RHI was administered on the stimulated hand. There was a significant difference between the embodiment and control statements ($p < 0.05$). For the right hand stimulation (Rhstim), the illusion statements *(Q1-Q3)* on the questionnaire received consistent responses (1.86 ± 0.30), whereas the control statements *(Q4-Q9)* received responses (-0.27 ± 0.23) at the 95% CI for a mean difference of (1.704, 2.56).

For the left hand stimulation (Lhstim), the illusion statements *(Q1-Q3)* on the questionnaire received consistent positive responses (1.89 ± 0.26), whereas the control statements *(Q4-Q9)* received responses (-0.20 ± 0.32) at the 95% CI for a mean difference of (1.32, 2.88). No significant differences were noted between right- and left-hand stimulation ($p > 0.05$), as shown in Figures 10 and 11.

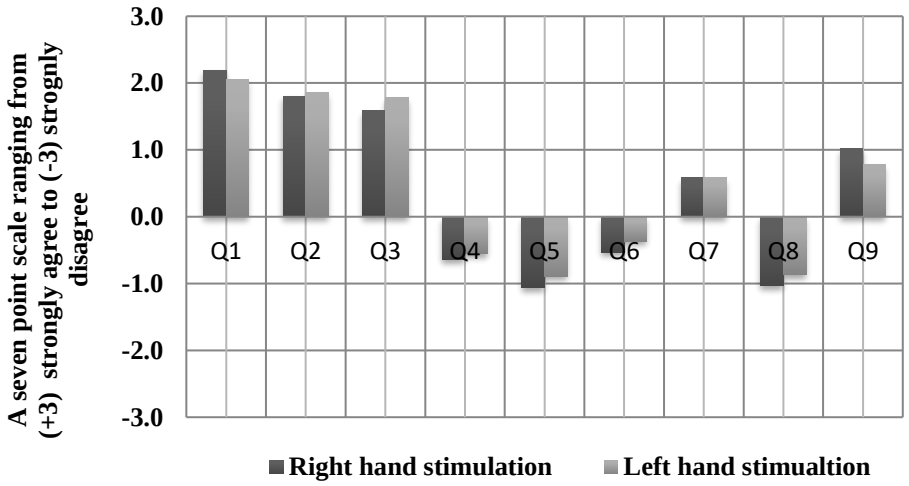

Figure 10: Overall Participant Responses for Right- and Left-Hand Stimulation.

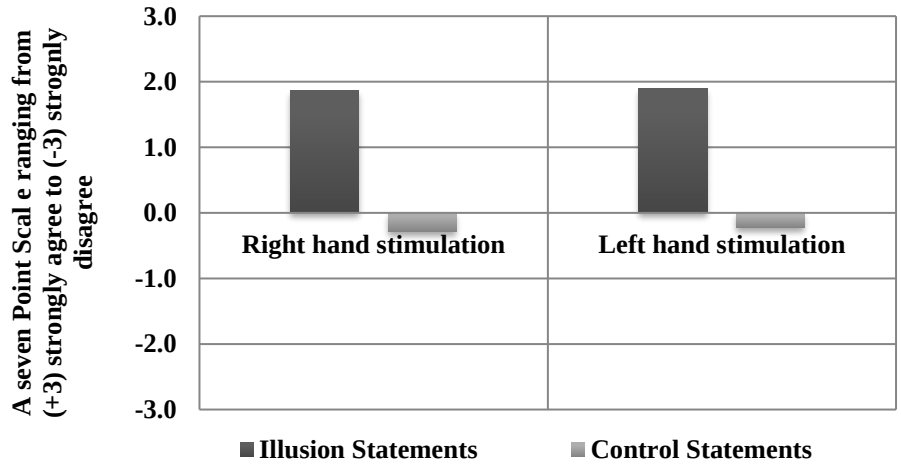

Figure 11: Comparison Between Right- and Left-Hand Stimulation.

3.6.2 Heart Rate

There was no significant difference in HR between BL (72.96 ± 2.55 bpm) and stimulation (71.57 ± 2.85 bpm) in the stimulated hand (p = 0.12) at 95% CI for a mean difference of (-0.44, 3.22) (Figure 12). A similar result was found when the left hand was stimulated (p = 0.29); BL (68.30 ± 2.36 bpm) and stimulation (68.90 ± 2.55 bpm) at 95% CI for a mean difference of (-1.81, 0.59).

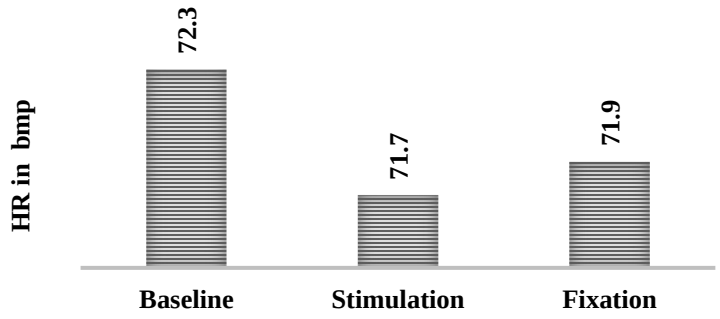

Figure 12: Overall Mean of Heart Rate.

3.6.3 Mean Arterial Pressure

There was no significant difference (p = 0.56) in the MAP between BL (94.18 ± 4.89 mm Hg) and stimulation (94.25 ± 5.15 mm Hg) in the stimulated right hand at 95% CI for a mean difference of (-1.78, 1.01) as well as when the left hand was stimulated (p = 0.35), BL (93.65 ± 3.45 mm Hg) and stimulation (94.29 ± 3.13 mm Hg) (Figure 13).

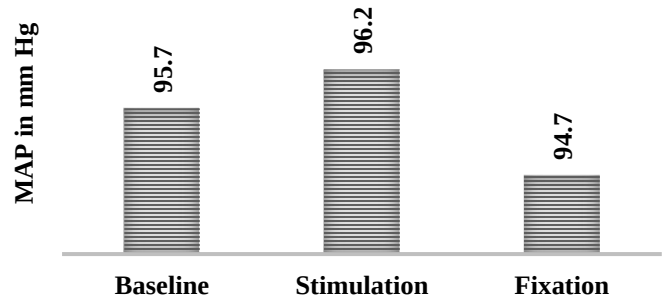

Figure 13: Overall Mean of Mean Arterial Pressure.

A negative correlation (-0.59) between overall means of MAP and HR (p = 0.002) was found.

3.6.4 Mean Blood Velocity

There was a significant difference in mean velocity (Vm) between BL (5.02 ± 0.45 cm/sec) and stimulation (4.37 ± 0.34 cm/sec) when the right hand was stimulated (Rhstim shown in Figure 16); p = 0.04 at 95% CI for a mean difference of (0.04, 1.26). No significant difference in Vm was found between BL (4.59 ± 0.72 cm/sec) and stimulation (5.13 ± 0.71 cm/sec) at 95% CI for a mean difference of (-1.84, 0.78) when the right hand was used as a control but the stimulation was applied to the left hand (p = 0.39) (RhCtrl shown in Figure 14).

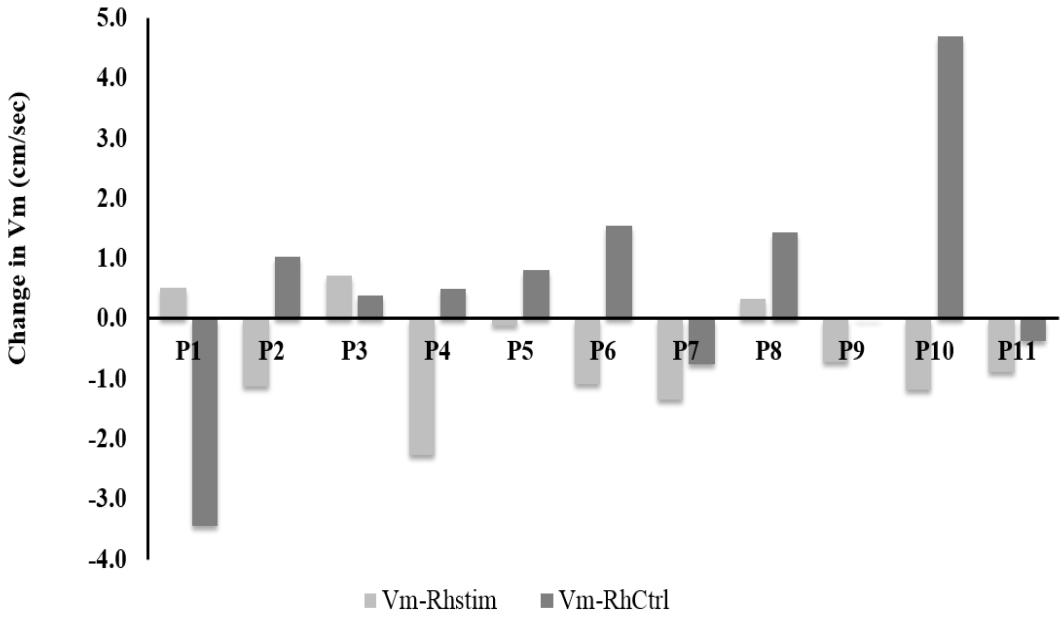

Figure 14: Comparison of Mean Velocity change relative to baseline between hands.

3.6.5 Doppler Blood Flow

We found a significant difference in DBF between BL (2.99 ± 0.27 ml/min) and stimulation (2.61 ± 0.20 ml/min) when the right hand was stimulated $p = 0.04$ at 95% CI for a mean difference of (0.02, 0.76). There was no significant difference in DBF between BL (2.74 ± 0.43 ml/min) and stimulation (3.06 ± 0.42 ml/min) when the right hand was used as a control and the stimulation was applied to the left hand ($p = 0.39$) at 95% CI for a mean difference of (-1.10, 0.46). These findings suggest that decreased DBF may have been an effect of the RHI (see Figures 15-16).

3.6.5.1 Doppler Vascular Conductance

To find DVC, DBF was calculated as shown in Eqs. 6 and 7. Value *approaching* a significant difference was found in DVC between BL (0.032 ±0.002 ml//min/mm Hg) and stimulation (0.027 ±0.002 ml//min/mm Hg) when the right hand was stimulated ($p = 0.054$) at 95% CI for a mean difference of (-0.00009, 0.0084). No significant difference was seen in DVC between BL (0.029 ±0.004 ml//min/mm Hg) and stimulation (0.033 ± 0.005 ml//min/mm Hg) when the right hand was used as a control and the stimulation was applied to the left hand ($p = 0.32$) at 95% CI for a mean difference of (-0.012, 0.0045).

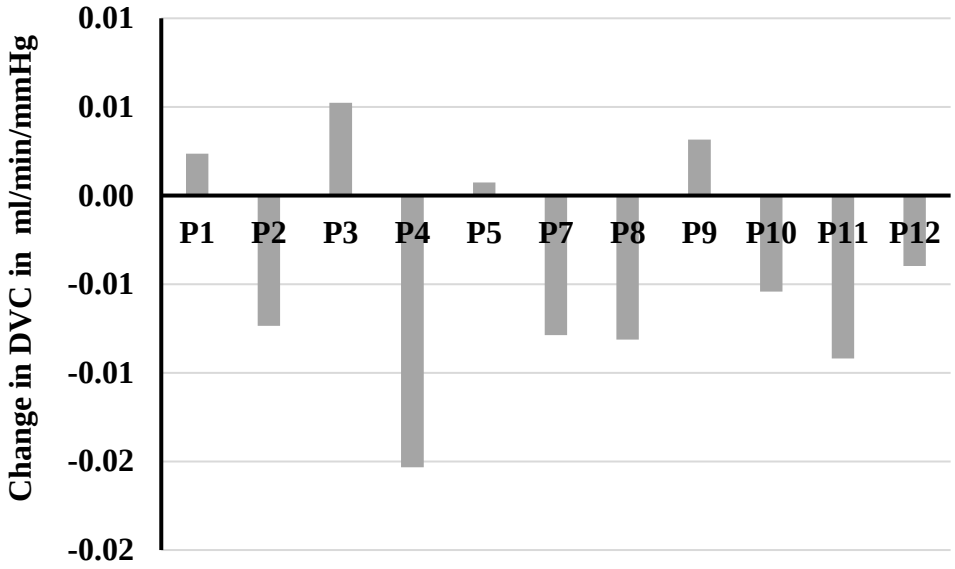

Figure 15: Doppler Vascular Conductance in the Stimulated Right Hand.

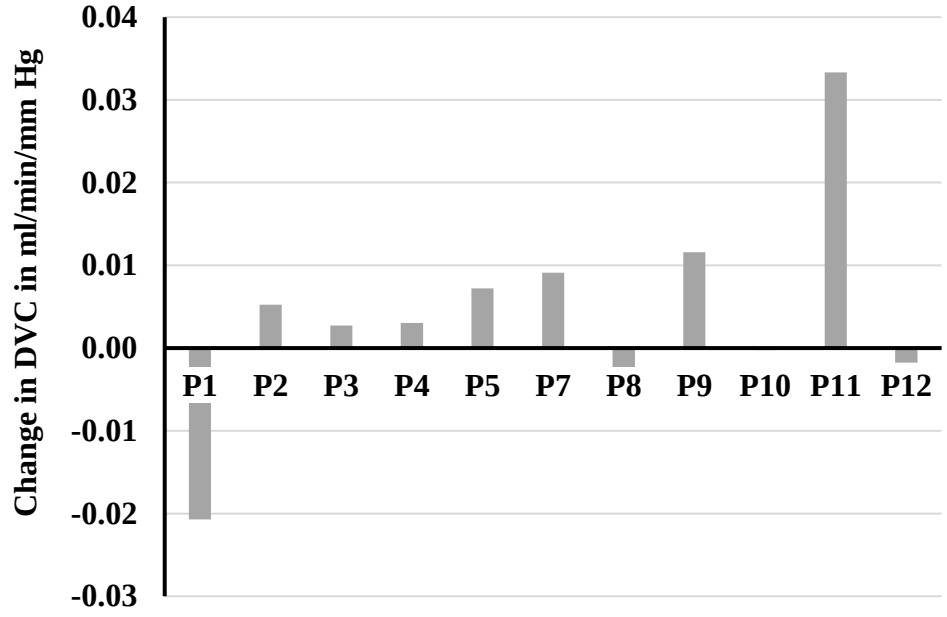

Figure 16: Doppler Vascular Conductance in the Control Right Hand.

3.6.5.2 Doppler Vascular Resistance

DVR was calculated as the inverse of DVC. No significant difference ($p > 0.05$) was found in the DVC between BL (35.40 ± 4.44 mmHg/ml/min) and stimulation (38.80 ± 3.05 mm Hg/ml/min) in the stimulation condition at 95% CI for a mean difference of (-10.36, 3.56). The BL (42.17 ± 5.44 mmHg/ ml/min) and stimulation (38.33 ± 5.89 mm Hg/ml/min) showed a 95% CI for a mean difference of (-5.64, 13.3) in the control condition.

3.6.6 Resistive Index (RI)

In the RI, there was no significant difference between BL and stimulation in either the stimulated hand (BL [0.86 ± 0.01] and stimulation [0.84 ± 0.01]) at 95% CI for a mean difference of (-0.02, 0.07), $p = 0.28$, or in the control hand (BL [0.78 ± 0.02] and stimulation [0.79 ± 0.02]) at 95% CI for a mean difference of (-0.04, 0.03), $p = 0.73$ (Figure 17, A and B).

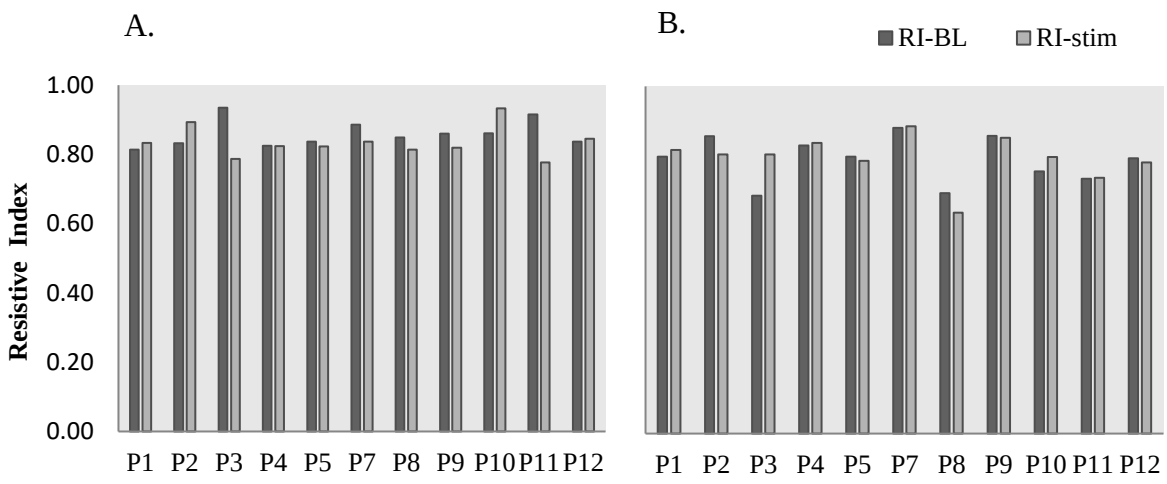

Figure 17: Resistive Index in the Right Stimulated (A) and Right Control (B) Hands.

3.6.7 Pulsatility Index (PI)

Similar findings held for the PI. There was no significant difference between BL and stimulation in either the stimulated or control hand: BL (5.04 ± 0.68) and stimulation (5.70 ± 0.61) at 95% CI for a mean difference of (-2.02, 0.69) in the stimulated hand (p = 0.30); BL (6.50 ± 1.59) and stimulation (5.95 ± 0.66) at 95% CI for a mean difference of (-2.20, 3.32) in the control hand (p = 0.66) (Figures 18-19).

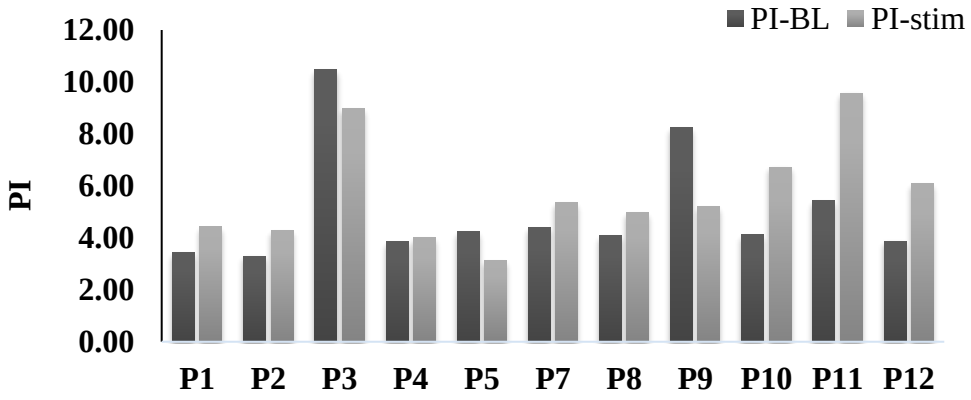

Figure 18: Pulsatility Index in the Stimulated Right Hand.

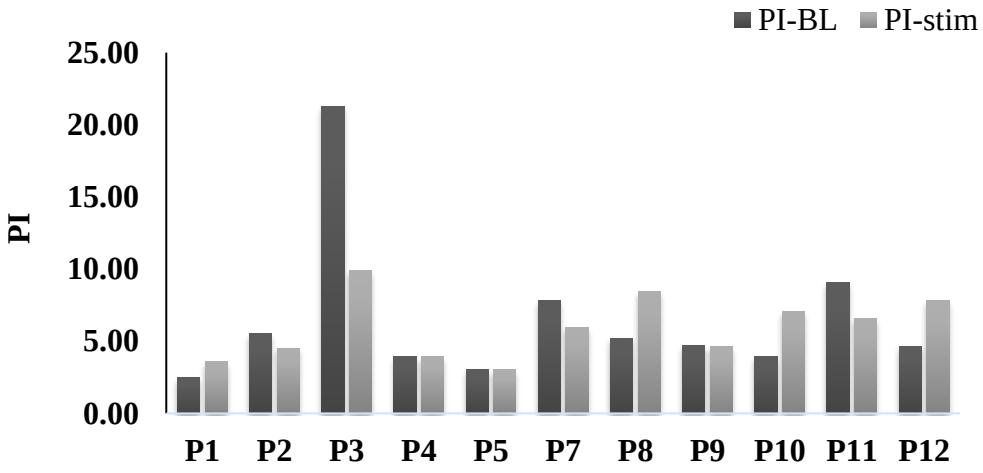

Figure 19: Pulsatility Index in the Control Right Hand.

3.7 Discussion

The motivation of this first study included three sub-aims: **(1)** develop a modified method that both allowed the induction of the RHI and an ultrasound system for measuring blood flow accurately; **(2)** quantify the relative change in volume flow in the given region per unit time; and **(3)** examine the hypothesis that the waveform indices RI and PI can be used as linking these waveform indices to physiological quantities such as vascular resistance.

3.7.1 Responses to Questionnaire

Although a few studies have investigated the link between laterality and strength of cognitive embodiment, a statistical comparison between both hands was not mentioned in terms of subjective differences between the right and left hand as reported by subjects. Our results suggest that handedness did not influence the strength of the illusion. The embodiment questionnaire data confirmed that there was no statistical difference between the right and left hand when investigating the effect of the RHI, suggesting that the brain representation for both hands is the same. This finding is consistent with what has been found in previous studies (Ocklenburg et al., 2011; Smit et al., 2017).

3.7.2 Blood Pressure and Heart Rate

It is well established that blood pressure and HR are associated and controlled by the SNS. Our results revealed a negative correlation (-0.59) between overall means of MAP and HR (p = 0.002). This suggests that when an increase in arterial pressure is detected, the PNS is activated to reduce HR and when a decrease in arterial pressures is detected, the SNS is activated to increase HR.

In this study, blood pressure was measured using a finger cuff on the third digit of the stimulated hand. It has been reported that blood pressure in the vessels decreases as the distance away from the heart increases (Berne et al., 2008). One limitation of our implementation is that it is unclear whether the RHI has a global or local effect on blood pressure. However, this effect does seem to depend on changes in vessel constriction and smooth muscle contraction.

We speculate that during the stimulation, there is an increase in peripheral resistance due to a reduction in the vessel diameter, thus an increase in blood pressure. Our findings on the effects of cognitive limb embodiment on blood pressure at least hint that the effects may be both local and global. To investigate the global effect, the blood pressure finger cuff should be placed on the control hand.

3.7.3 Blood Flow Velocity and Vascular Conductance

There is no previous research using Doppler ultrasound to measure blood flow under the condition of the cognitive illusion. A new approach was therefore needed. For this study, it was of interest to use the modified ultrasound approach to quantify the relative changes in the blood flow at the brachial artery.

With this aim in mind, we present a modified ultrasound method that consists of the following aspects: DG of 1.3 mm, Doppler angle (θ) of 60°, and DL. By doing so, the blood velocity and blood flow may offer similar information. However, it is important to note that blood flow information is needed to estimate other hemodynamic parameters, such as vascular conductance. The data obtained from blood flow velocity measurements convey important information regarding the physiological processes.

Our data showed that blood flow velocities in the brachial artery decreased significantly during the stimulation (p = 0.04). This result ties in well with a previous study, wherein blood flow was reduced in both brachial and radial arteries; it was argued that this reduction may be related to increased peripheral resistance because of the reduction in the sympathetic tone (Takayama et al., 2012).

As blood flow velocity is directly related to vessel diameter; when the vessel become smaller, the flow velocities are reduced. Thus, the reduction in Vm in the stimulated hand may be caused by the RHI, as the control hand showed an increase in mean velocity. Regarding the vascular conductance results, we found a *marginally* significant difference (p = 0.045) between BL and stimulation during the stimulation condition. This finding suggests that the decreased blood flow appears to be due to a lower vascular conductance that is associated with the RHI, as there was no difference in the vascular conductance in the control condition.

3.7.4 Doppler Waveform Indices

Blood circulation is founded on a pulsatile system, in which velocity distribution and waveform indices are continuously changing. Data obtained from the Doppler waveform indices PI and RI provide helpful information to better understand the relationship between these hemodynamic parameters. It is known that pressure differences in the vessel and resistance to flow are the main factors affecting blood flow (Nelson and Pretorius, 1988). From the blood flow measurements, one can speculate about the role of peripheral resistance.

It is established that arterioles play a vital role for determining peripheral resistance (Chavhan et al., 2008). One can hypothesize that since vessel diameter is a key determinant for peripheral vascular resistance, small changes in vessel diameter lead to large changes in resistance. Therefore, no significant differences were found in the PI and RI results in either the stimulated or control hand.

An important point to keep in mind is that the Doppler information is obtained from the DG (sampling volume within the blood vessel) and not from the entire vessel diameter. Since changes in arterial resistance occur from variations in blood-vessel diameter (Hoskins et al., 2017), the changes in resistance within the DG size of 1.3 might be too small to be detected. This may explain why there were no statistical differences in RI and PI in our results.

CHAPTER IV

THE LINK BETWEEN TEMPERATURE AND BLOOD FLOW

4.1 Introduction

Recently, several studies have established a correlation between the induction of the RHI and skin surface temperature changes in healthy individuals (Moseley et al., 2008; Kammers et al., 2011). Interestingly, when a limb becomes disembodied during the cognitive illusion, the temperature of that limb drops. This literature suggests that through the cognitive mechanism of visual-tactile integration, the brain can derive body representation and determine that the rubber hand belongs to the participant (Ehrsson et al., 2008; Tsakiris, 2010; Ratcliffe and Newport, 2017). It has been reported that the change in skin temperature between the upper limbs is a physiological correlate for the RHI effect (Ramakonar et al., 2011; Rohde et al., 2013). A study from our lab has demonstrated a link between the RHI and reduction in skin temperature with above-elbow amputees (Marasco et al., 2011).

Although it is evident that the RHI may manifest both cognitively and physiologically, some reports in the literature suggest there is no link between skin temperature and the RHI. Several studies have failed to reproduce the effect of the RHI on skin temperature (Paton et al., 2012; Rohde et al., 2013; de Haan et al., 2017). One can question whether differences in the experimental procedures contributed to these conflicting findings, or whether the effect is so small that the noise in measuring it is greater than the effect itself. Our aim here is not to challenge these findings nor to conduct a validation study to scrutinize these findings; such a task is beyond the scope of this thesis. However, here we speculate on some of the factors that could be involved to elicit the effect of the RHI.

Factors associated with the temperature discrepancy results may be due to differences in the site of measurements, the selected regions or *"spots"* at which the temperature values were recorded, and the instruments that were used to measure the temperature. Differences in skin structure between palmar and dorsal sites might be the reason for temperature variation; the palmar side of the hand is rich in arteriovenous anastomoses (AVAs), known for their role in thermoregulation, whereas these AVAs are absent in the dorsum of the hand and are few in the dorsal side of the fingers (Gardner-Medwin et al., 1997). Therefore, different sites of measurements may yield variable results.

Investigating blood perfusion and whole-hand thermography (from the wrist down to the fingertips) can provide insights into the mechanisms of the RHI's physiological correlates. This approach may further establish quantitative measures to capture the embodiment experience, enabling a better understanding of the mechanisms

that contribute to body representation. The control of blood flow throughout human skin is of vital importance in the regulation of temperature. The link between skin temperature and the RHI has been investigated. Yet the connection between skin surface temperature and skin blood flow changes under the effect of the cognitive embodiment has not been established.

Measuring blood flow is clinically important because it can be used as a physiological measure of cognitive limb embodiment and may also be predominantly important in diagnosing disease states. It is hypothesized that blood flow in a specific limb can be disrupted by disrupting the sense of embodiment. Hence, the goal of this study was to investigate the relationship between skin surface temperature and skin blood flow at the upper limbs, based on the central hypothesis that cognitive embodiment affects skin blood flow.

To achieve this goal, three different modalities were combined: First, a physiological infrared thermal imaging system was used to capture the variations in limb skin temperature throughout the entire experiment. Second, NIRS was used to measure the amount of blood that actually flows through the capillaries of the vascular bed on the examined area in the forearm. Third, LDF was used to measure skin blood flow in the hand.

4.2 Methods

4.2.1 Participants

Twelve healthy volunteers (7 male, 5 female; all right-handed (one ambidextrous); age range from 23-48 years; mean ± SD 30.3 ± 9.01 years) were

recruited. This study was approved by Cleveland Clinic's Institutional Review Board (CCF IRB#14-402). Written informed consent was obtained from each subject prior to participation.

4.2.2 Experimental procedure

For each participant, three trials for each hand were performed. Three testing periods were conducted: Baseline (BL, 2 min), Visual Tactile Stimulation (VTS, 6 min), and Visual Fixation (VF, 2 min), as shown in Figure 20. The experimental setup and induction of the RHI were similar to the protocol followed in the first study.

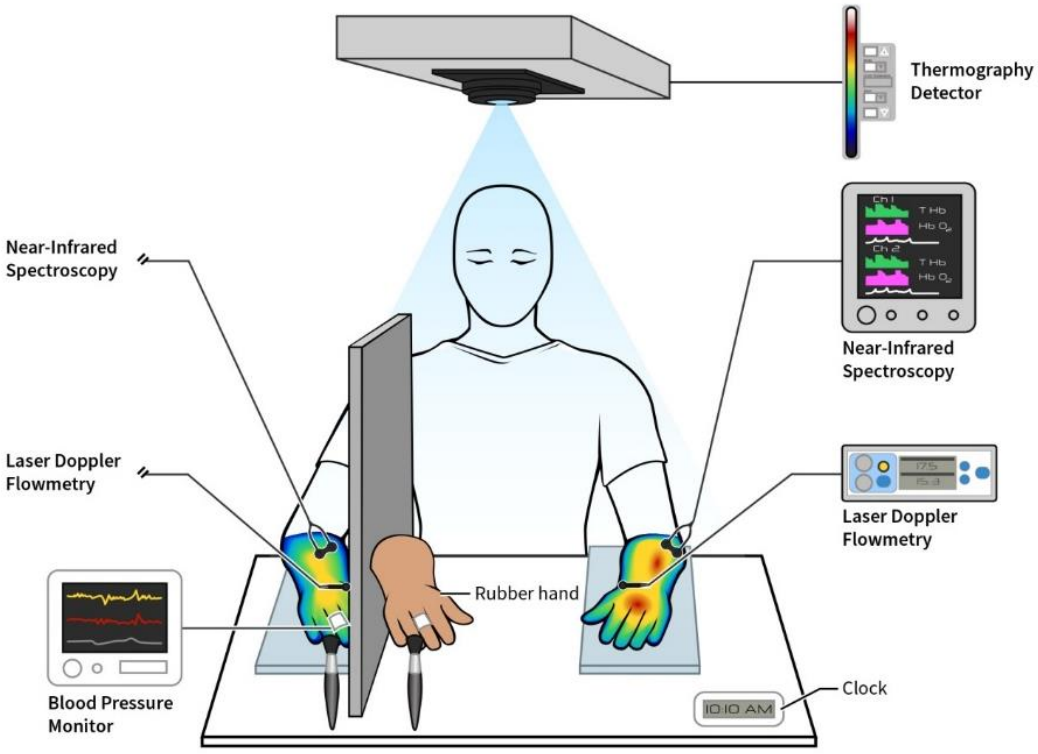

Figure 20: Experimental Setup for Investigating Temperature and Blood Flow.

4.2.3 Measuring Skin Surface Temperature Using Thermography

A Meditherm camera (Meditherm, Inc., Cheyenne, WY) was positioned facing downward with a field of view that focused to include both real hands of the participant. Skin surface temperature measurements on both stimulated and control hands were evaluated continuously throughout the experiment to ensure accuracy and reliability.

The Meditherm camera works by converting infrared radiation emitted from the skin surface into electrical impulses that are visualized in color on a computer monitor. This visual image graphically maps body temperature, and these data can be stored as images. The files can then be manipulated with MATLAB image processing software (MathWorks, Natick, MA).

To compute temperature, two customized MATLAB codes were developed. The first MATLAB code was used to compute temperature with a linear model: $y = m * x + b$, and $m = \frac{Tmax - Tmin}{18}$ and $b = Tmin - m$. The minimum temperature (Tmin) and maximum temperature (Tmax) were documented from the image data (Table 3). The second MATLAB code was used to run data from all images for a trial as one sequence image after selecting the regions of interest on both hands, as shown by the white dotted lines in Figure 21. It should be noted that the black background was eliminated to ensure proper mean temperature measurement.

Table 3: Temperature Collected from Image Data.

Participant	Maximum temperature (°C)	Minimum temperature (°C)
1	33.5	25.5
2	35.0	27.0
3	32.2	24.2
4	32.2	25.2
5	32.3	24.3
6	33.4	25.4
7	33.3	25.3
8	32.2	24.2
9	31.3	23.3
10	31.1	25.1
11	33.0	25.0
12	34.0	26.0

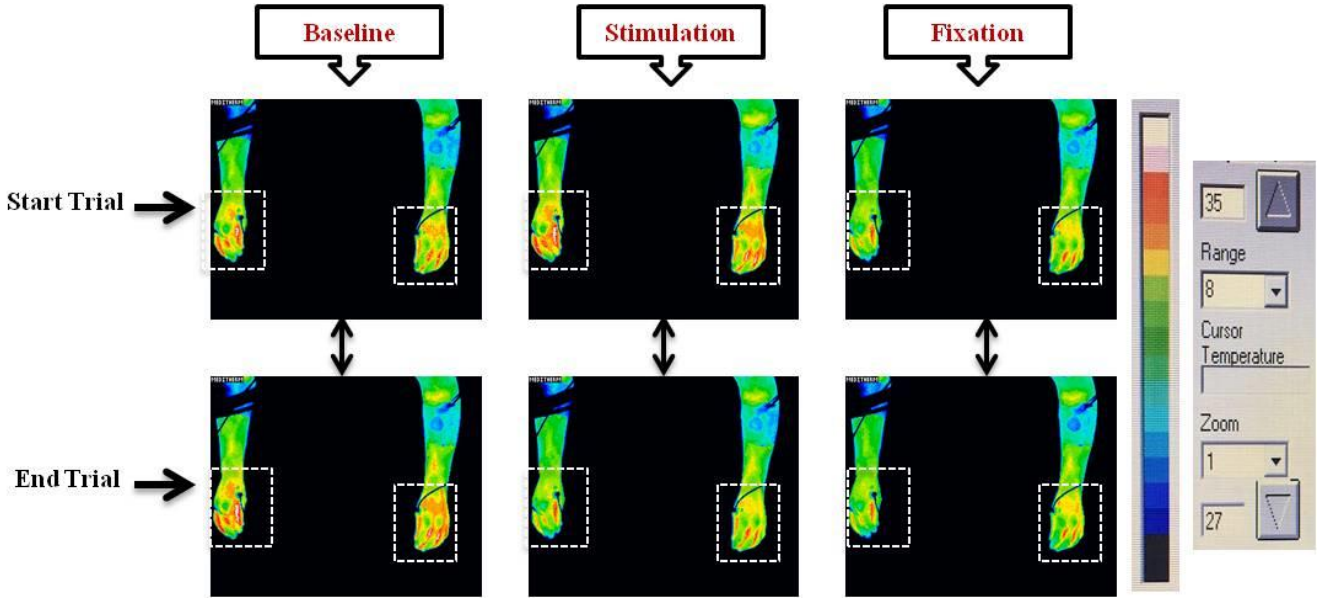

Figure 21: Temperature Data Collection.

4.2.4 Calculating Skin Blood Flow Using Laser Doppler Flowmetry

LDF is a noninvasive technique that can be used to measure relative changes in microcirculatory blood perfusion (also known as flux). The governing principles of LDF are adapted from the light-wave theory described by Christian Doppler (Tabrizchi and Pugsley, 2000), in which a beam of laser light was led by a fiberoptic probe onto the tissue being examined. When the laser light hits moving blood cells, it is reflected (bounced back) with a different wavelength than the emitted wavelength; this change in wavelength is called the Doppler shift. The magnitude and frequency of the Doppler shift is directly related to the number of moving red blood cells and their velocity in the area being examined (also known as sample volume).

LDF **(**moorVMS-LDF2, Moor Instruments Inc., Wilmington, DE) was used. LDF probes were attached to the skin with double-sided adhesive patches. Both probes were connected to a dual-channel LDF system to allow simultaneous monitoring of the two limbs. Each probe was attached to the hand on the dorsal surface between the thumb and the index finger. Disadvantages of LDF are that the testing area is small, and flowmetry cannot measure the absolute skin blood flow in a region. LDF measurements are expressed as perfusion units, which are arbitrary. Vascular conductance was calculated as LDF/MAP.

The site of measurement plays a critical role in determining the characteristics of flux; for example, flux at the palmar sites of the hand is prominent. This is because, at the palmar site, flux would be consistent with high flow of the AVAs in the vessels, with fewer AVAs at the dorsal sites on the hand (Gardner-Medwin et al., 1997).

4.2.5 Estimating Tissue Blood Flow Using Near-Infrared Spectroscopy

NIRS is a noninvasive technique that uses the different dynamic absorption patterns of near-infrared light in oxygenated and deoxygenated hemoglobin to estimate blood flow (Casey et al., 2008; Abay and Kyriacou, 2016). An NIRS oxygenation monitor (NIRO-200NX, Hamamatsu Photonics, Bridgewater, NJ) was used. NIRS has commonly been used as a real-time monitor of tissue oxygenation in many clinical and research settings. The NIRS probe has two light-emitting sensors generating two different wavelengths: red, 730 nm, and infrared, 810 nm (Boezeman et al., 2014).

It has been reported that, to maintain tissue oxygenation, microcirculation has to direct sufficient blood flow to the tissue with higher metabolic needs (Jacob et al., 2016). The probes were attached to the skin with a probe holder and double-sided adhesive patches; they were covered with medical tape to occlude light to cancel out possible noisy data. Each probe was attached to a hand on the dorsal forearm. To allow simultaneous monitoring of tissue blood flow, both probes were connected to the dual channels of the NIRS.

4.3 Statistical Analysis

MATLAB software (MathWorks) was used to pre-process thermographic images; then mean temperature values for both right and left hands were calculated. Minitab software 17 (Minitab Inc.) was used for statistical analysis. A repeated-measures analysis of variance (RM-ANOVA) for mean temperature response with Bonferroni correction for multiple comparisons was used. A paired *t* test was used to compare the relative changes

in mean temperature between conditions (e.g., BL, VTS, and VF). A nonparametric Wilcoxon signed rank test was used for non-normally distributed data.

4.4 Results

4.4.1 Skin surface temperature

There was a significant difference in mean temperature between the stimulated and control hands when using RM-ANOVA (p = 0.009), as illustrated in Figure 22. No significant difference was found between the conditions (BL, VTS, and VF, $p > 0.05$), as shown in Figure 23. A significant difference in mean temperature was found between the stimulated and control hands (p = 0.001) when using the Bonferroni pairwise for multiple comparisons with 95% confidence; the mean temperature for the right stimulated hand (28.71°C) and for the control hand (29.60°C). There was no significant interaction between (Hand *condition), $p > 0.05$.

In addition, a paired t test was conducted to investigate the mean temperature differences between BL and stimulation conditions in all trials. There was no significant difference ($p > 0.05$) in the mean temperature; the BL was (28.67 ± 0.47°C) and stimulation (28.56 ± 0.43°C) during the stimulation condition; at 95% CI for a mean difference of (-0.12, 0.34).

In the control condition, we obtained BL (29.51 ± 0.39 °C) and stimulation (29.56 ± 0.34 °C) values at 95% CI for a mean difference of (-0.36, 0.26). It should be noted that we collected mean temperature values when the left hand was stimulated. There was no significant difference in the mean temperature ($p > 0.05$). These data were not included in this study analysis.

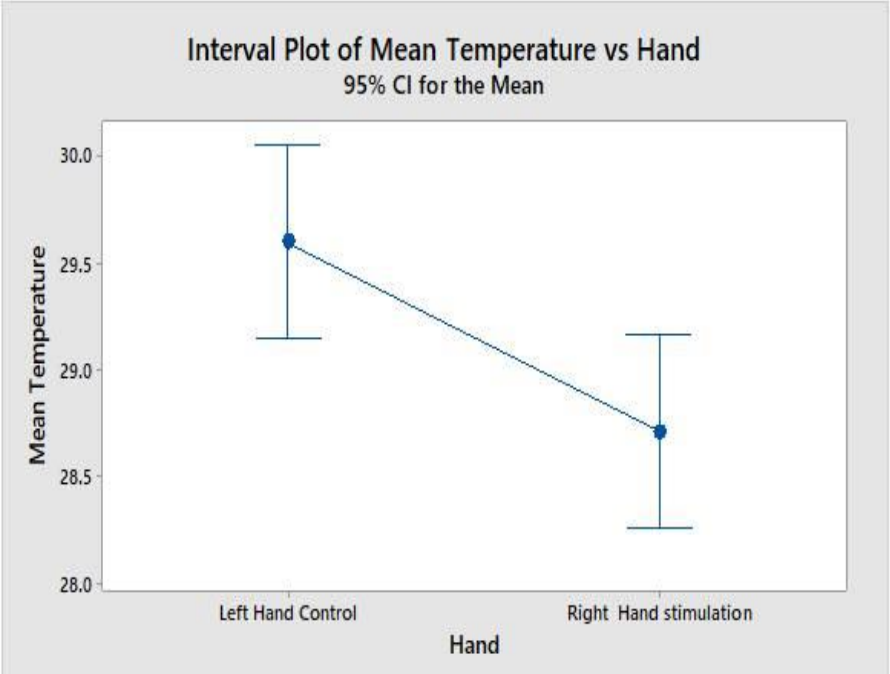

Figure 22: Temperature and Stimulation.

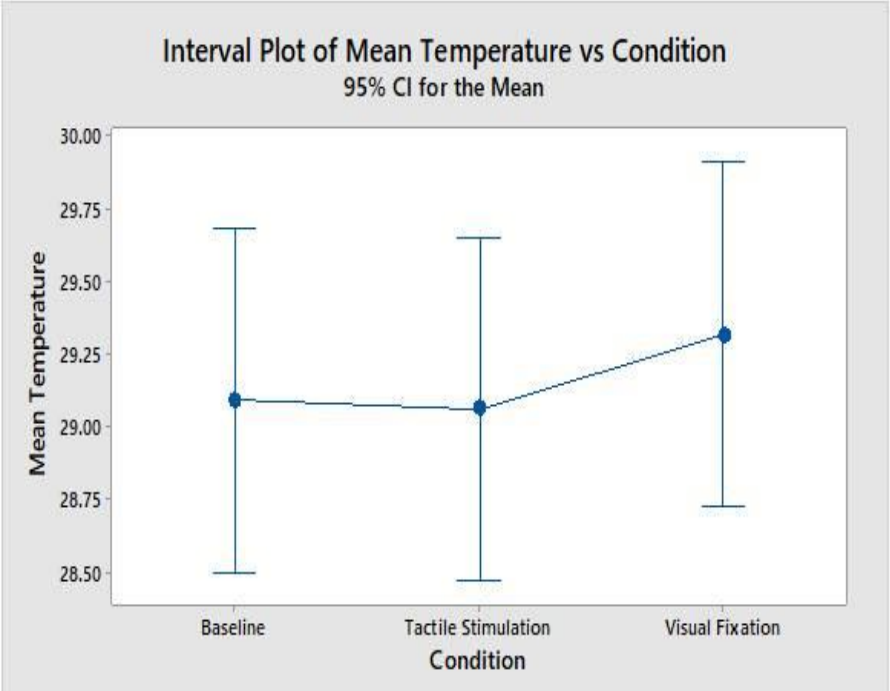

Figure 23: Temperature and Conditions in the Stimulated Right Hand.

4.4.2 Skin Blood Flow

Data were not normally distributed; therefore, a Wilcoxon Signed Rank test on two paired samples was used. There was a significant difference in skin blood flow on the stimulated hand (Z = -2.045, p = 0.041). The W-value is 10. The critical value of W for N = 11 at $p \leq 0.05$ is 10. Therefore, the result is significant at $p \leq 0.05$. There was no significant difference for the left hand control ($p > 0.05$). There was no significant difference when the left hand was stimulated and the right hand was used as a control ($p > 0.05$).

4.4.2.1 Laser Doppler Flowmetry—Conductance

There was a significant difference in skin LDF-conductance on the stimulated hand (Z = -2.31, p = 0.02). The W-value is 7. The critical value of W for N = 11 at $p \leq 0.05$ is 10. Therefore, the result is significant at $p \leq 0.05$. There was no significant difference for the left control hand ($p > 0.05$). There was no significant difference when the left hand was stimulated and the right hand was used as a control ($p > 0.05$). The interaction between the conditions showed no significant difference ($p > 0.05$) in either left or right hand, as illustrated in Figures 24 and 25.

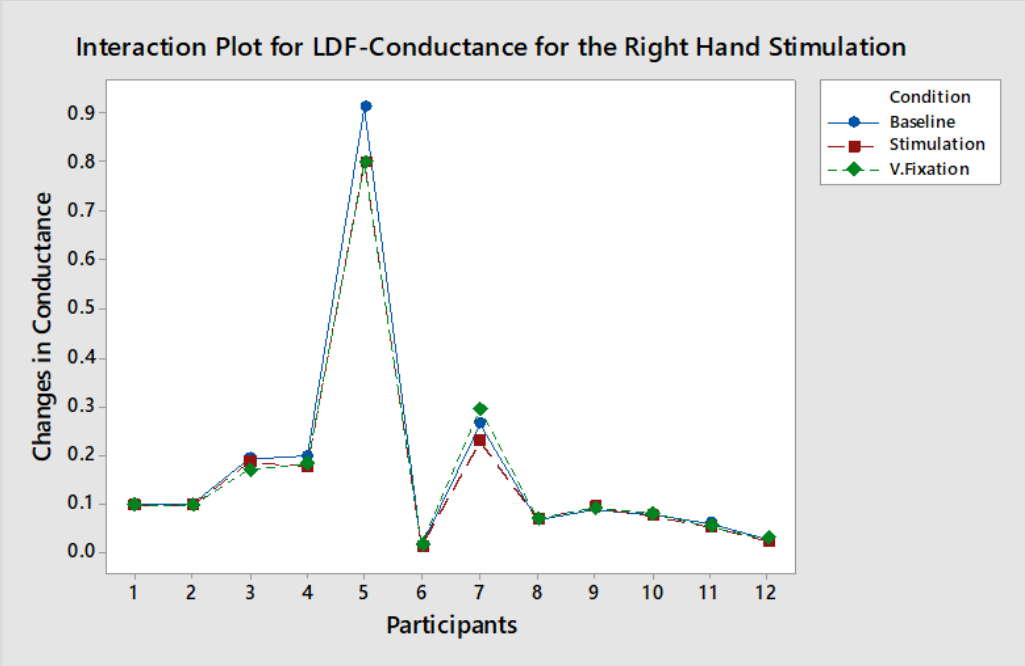

Figure 24: Stimulated Hand LDF-Conductance

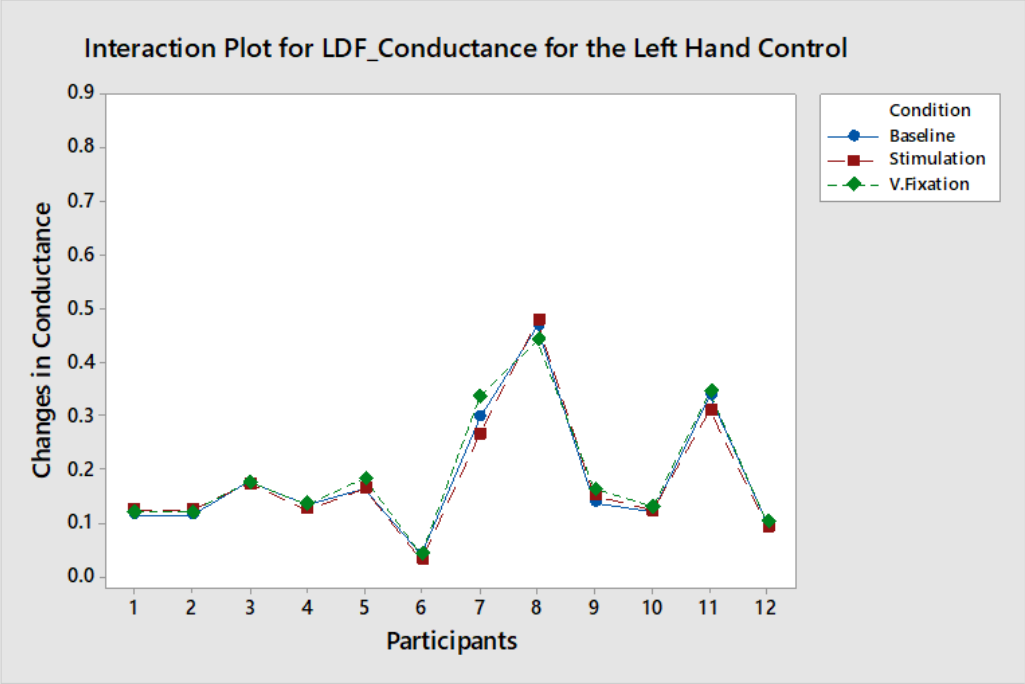

Figure 25: Control Hand LDF-Conductance

4.4.3 Tissue Blood Flow

For oxygenated hemoglobin (OHB), there was no significant difference in tissue blood flow on the right stimulated hand (Z = -1.68, p = 0.09) and no significant difference for the left control hand (p = 0.60). A difference *approaching* significance was found when the left hand was stimulated and the right hand was used as a control (p = 0.05).

For total hemoglobin (THB), there was no significant difference in tissue blood flow on the right stimulated hand (Z = -1.88, p = 0.06) and no significant difference for the left control hand (p = 0.80). There was no significant difference when the left hand was stimulated and the right hand was used as a control ($p > 0.05$).

4.5 Discussion

The motivation of this second study was to investigate the link between temperature and blood flow changes during the RHI by using three physiological measures on different measurement sites: a physiological infrared thermal imaging system to capture variations in skin temperature in the dorsal side of the hand; LDF to measure the skin blood flow in the hand (in the dense tissue area between the thumb and the index finger); and NIRS to measure tissue blood flow in the forearm.

4.5.1 Skin Surface Temperature

Here, we used infrared thermography to measure the mean temperature in the dorsal side of the hand from the wrist to the fingertips. As expected, a significant difference was found in mean temperature between the stimulated and the control hands. These results are in line with those of previous studies.

From our own work, it is established that changes in skin temperature are related to the RHI-facilitated limb cognitive embodiment (Marasco et al., 2011). It has been reported that the RHI induces a decrease in hand temperature of about one fourth of a degree (Moseley et al., 2008). However, the relative changes in mean temperature between the conditions (BL, VTS, and VF) were expected to be too small to be detected. Therefore, we documented no statistical difference between conditions. We found a statistical difference on the stimulated but not the control hand, as our mean temperature data confirmed that. Therefore, the most likely explanation is that this is due to the effect of the RHI on physiological responses such as changes in temperature and blood flow that occur due to disembodiment of the actual limb and embodiment if the rubber hand. To conclude, the difference in mean temperature during the stimulation showed the effect of the RHI.

4.5.2 Skin Blood Flow

Our results showed a significant difference in skin blood flow and skin LDF-conductance in the stimulated hand, with no significant difference for the control hand. From a study that investigated changes in blood flow using LDF, it is confirmed that LDF-flux can be used as an indicator of reduction in blood flow due to vasoconstriction (Abay and Kyriacou, 2016). This may suggest that skin blood flow (and thus LDF-conductance), reduced on the stimulated hand, is due to the decrease in vessel diameter caused by the effect of the RHI.

4.5.3 Tissue Blood Flow

For tissue blood flow, the relative changes in the amount of oxygenated hemoglobin and total hemoglobin in the dorsal forearm were not significant between the stimulated and the control hand. One explanation might be that the rate of blood flow is slowest in the capillaries to allow time for the exchange of gases and nutrients. In addition, blood flow differs inversely with the total cross-sectional area of the blood vessels; as the total cross-sectional area of the vessels increases, flow decreases. This may explain why our tissue blood flow findings showed no statistically significant difference. Furthermore, when comparing forearm to the hand to the finger tips, blood flow may vary, depending on the vascular anatomy of the skin. For instance, the number of AVAs present in the forearm is less than those in the hand. It has been reported that blood flow in the forearm plays no major thermoregulatory role as the AVAs are fewer (Johnson et al., 1986). The same conclusion was confirmed by another study of blood flow in different locations; investigators found that the blood flow in the fingertips is the highest but lowest in the forearm (Ikawa and Karita, 2015).

CHAPTER V

CONCLUSIONS AND FUTURE WORK

5.1 CONCLUSIONS

Although the technique to induce the RHI is simple, the cognitive physiological responses are profound. Our findings support the central hypothesis that blood flow in a specific limb can be altered by disrupting the sense of embodiment. The main conclusion that can be drawn is that the decreased blood flow appears to be due to a lower vascular conductance that is associated with the RHI effect.

To our knowledge, this study is the first study to use the Doppler ultrasound technique to measure the relative changes in blood flow under the effect of cognitive embodiment in a healthy population. Therefore, there was a need to develop a new approach by both modifying the standard ultrasound method to measure blood flow while ensuring the induction of the illusion to meet the main goal of this work. However, the limitations of the present approach naturally include factors such as participants'

movement and fatigue due to the comprehensive investigation. As we have argued elsewhere, our modified approach hold a promising aspect of blood-flow measurement under the effect of cognitive embodiment. Ideally, these findings should be replicated in a study where the goal is to investigate the relative changes in blood flow rather than the net flow under the effect of external stimuli. Our results have significant implications for individuals' health as it relates to both cognitive and physiological responses.

In the second study, we found a reduction in mean temperature and skin blood flow in the stimulated hand. There has not been an investigation to combine all three of these blood-flow-monitoring modalities to examine thermal and vascular changes under the condition of cognitive embodiment. Our results of this second study support our hypothesis that there is a link between skin temperature and blood flow.

The overall hypothesis for this study was that the blood flow can be altered by the sense of cognitive embodiment. From previous literature, it is evident that the RHI may manifest both cognitive and physiological effects. Taking our data altogether, these results confirmed our hypothesis and showed that disruption of blood flow can be attributed to the effects of the RHI.

5.2 FUTURE WORK

With the success of our investigation in finding a link between the RHI and vascular changes, we realized the power of cognitive illusions can be used as a technique to provide useful information about the characteristics of vessel constriction under an external stimulus. Importantly, this line could lead us to another very interesting research focus point that encouraged us to ask whether there is an association between vessel constriction and the strength of the illusion. Thus, the next focus of research attention could be on capturing changes in vessel diameter during cognitive limb embodiment with the aim of investigating the potential relationship between the strength of the illusion and the magnitude of vessel-diameter constriction.

To obtain accurate vessel-diameter measurements, several steps should be considered. Data could be recorded and saved as sequential image clips in the ultrasound system. Images then can undergo post-processing (e.g., edge-detection techniques) to identify the regions of interest, and measures of vessel diameter can be taken for further analysis. We anticipate that the strength of the RHI will correlate with changes in vessel diameter: the more strongly the participant feels the illusion, the greater the reduction in vessel diameter.

Current microcirculation studies have used vessel-diameter measurements to gauge the effects of various stimuli (Lee et al., 2009). As has been reported in the literature, peripheral vasoconstriction may be caused by sympathetic stimulation (Archer et al., 1984). Yet there is no research investigating the link between vessel constriction and cognitive limb embodiment.

Capturing blood-flow characteristics offers a better understanding of vascular physiological changes because changes in vascular perfusion may reflect a physiological response such as thermoregulation or a pathologic response. For instance, alteration of blood flow is one of the main causes of diabetic complications (Argoff et al., 2006; Bagavathiappan et al., 2010), which often lead to ulceration and amputation (Sumpio, 2000; Feng et al., 2009).

Further extensions of this work may help not only to unlock improved mechanistic understandings of the underlying metabolic changes such as in diabetes but also to determine new avenues for therapeutic intervention.

REFERENCES

Abay TY, Kyriacou PA (2016) Comparison of NIRS, laser Doppler flowmetry, photoplethysmography, and pulse oximetry during vascular occlusion challenges. Physiol Meas 37:503–514.

Archer AG, Roberts VC, Watkins PJ (1984) Blood flow patterns in painful diabetic neuropathy. Diabetologia 27:563–567.

Argoff CE, Cole BE, Fishbain DA, Irving GA (2006) Diabetic peripheral neuropathic pain: clinical and quality-of-life issues. Mayo Clin Proc 81(4 Suppl):S3-11.

Bagavathiappan S, Philip J, Jayakumar T, Raj B, Rao PNS, Varalakshmi M, Mohan V (2010) Correlation between plantar foot temperature and diabetic neuropathy: a case study by using an infrared thermal imaging technique. J Diabetes Sci Technol 4:1386–1392.

Berg S, Torp H, Haugen BO, Samstad S (2000) Volumetric blood flow measurement with the use of dynamic 3-dimensional ultrasound color flow imaging. J Am Soc Echocardiogr 13:393–402.

Berne RM, Levy MN, Koeppen BM, Stanton BA, eds. (2008) Berne & Levy Physiology. 6th ed. Philadelphia: Mosby/Elsevier.

Blanco P (2015) Volumetric blood flow measurement using Doppler ultrasound: concerns about the technique. J Ultrasound 18:201–204.

Boezeman RP, Kelder JC, Waanders FG, Moll FL, de Vries JP (2014) In vivo

measurements of regional hemoglobin oxygen saturation values and limb-to-arm ratios of near-infrared spectroscopy for tissue oxygenation monitoring of lower extremities in healthy subjects. Med Devices Evid Res (Auckland) 8:31-36.

Botvinick M, Cohen J (1998) Rubber hands “feel” touch that eyes see. Nature 391:756

Calamante F, Thomas DL, Pell GS, Wiersma J, Turner R (1999) Measuring cerebral blood flow using magnetic resonance imaging techniques. J Cereb Blood Flow Metab 19:701–735.

Casey DP, Curry TB, Joyner MJ (2008) Measuring muscle blood flow: A key link between systemic and regional metabolism. Curr Opin Clin Nutr Metab Care 11:580–586.

Chami HA, Keyes MJ, Vita JA, Mitchell GF, Larson MG, Fan S, Vasan RS, O’Connor GT, Benjamin EJ, Gottlieb DJ (2009) Brachial artery diameter, blood flow and flow-mediated dilation in sleep-disordered breathing. Vasc Med 14:351–360.

Chavhan GB, Parra DA, Mann A, Navarro OM (2008) Normal Doppler spectral waveforms of major pediatric vessels: specific patterns. Radiographics 28:691–706

Colberg SR, Parson HK, Nunnold T, Holton DR, Swain DP, Vinik AI (2005) Change in cutaneous perfusion following 10 weeks of aerobic training in Type 2 diabetes. J Diabetes Complications 19:276–283.

de Galan BE, et al.; ADVANCE Collaborative Group (2009) Cognitive function and risks of cardiovascular disease and hypoglycaemia in patients with type 2 diabetes: The Action in Diabetes and Vascular Disease: Preterax and Diamicron Modified Release

Controlled Evaluation (ADVANCE) trial. Diabetologia 52:2328–2336.

de Haan AM, Van Stralen HE, Smit M, Keizer A, Van der Stigchel S, Dijkerman HC (2017) No consistent cooling of the real hand in the rubber hand illusion. Acta Psychol (Amst) 179:68–77.

Ehrsson HH (2005) Touching a Rubber Hand: Feeling of Body Ownership Is Associated with Activity in Multisensory Brain Areas. J Neurosci 25:10564–10573.

Ehrsson HH, Rosén B, Stockselius A, Ragnö C, Köhler P, Lundborg G (2008) Upper limb amputees can be induced to experience a rubber hand as their own. Brain 131(Pt 12):3443–3452.

Evans DH (1985) On the measurement of the mean velocity of blood flow over the cardiac cycle using Doppler ultrasound. Ultrasound Med Biol 11:735–741.

Feng Y, Schlösser FJ, Sumpio BE (2009) The Semmes Weinstein monofilament examination as a screening tool for diabetic peripheral neuropathy. J Vasc Surg 50:675-82, 682.e1.

Fischer MJM, Uchida S, Messlinger K (2010) Measurement of meningeal blood vessel diameter in vivo with a plug-in for ImageJ. Microvasc Res 80:258–266.

Gardner-Medwin JM, Taylor JY, Macdonald IA, Powell RJ (1997) An investigation into variability in microvascular skin blood flow and the responses to transdermal delivery of acetylcholine at different sites in the forearm and hand. Br J Clin Pharmacol 43:391-397.

Gill RW (1985) Measurement of blood flow by ultrasound: Accuracy and sources of

error. Ultrasound Med Biol 11:625–641.

Giummarra MJ, Gibson SJ, Georgiou-Karistianis N, Bradshaw JL (2008) Mechanisms underlying embodiment, disembodiment and loss of embodiment. Neurosci Biobehav Rev 32:143–160.

Hanamura K, Tojo A, Kinugasa S, Asaba K, Fujita T (2012) The resistive index is a marker of renal function, pathology, prognosis, and responsiveness to steroid therapy in chronic kidney disease patients. Int J Nephrol 2012:139565.

Hiltawsky KM, Wiegratz A, Enderle MD, Ermert H (2003) Real-time detection of vessel diameters with ultrasound. BiomedTechnik (Berl) 48:141–146.

Holowatz LA, Kenney WL (2010) Peripheral mechanisms of thermoregulatory control of skin blood flow in aged humans. J Appl Physiol (1985) 109:1538–1544.

Hoskins PR (1990) Measurement of arterial blood flow by Doppler ultrasound. Clin Phys Physiol Meas 11:1–26.

Hoskins PR, Lawford P V., Doyle BJ, eds. (2017) Cardiovascular Biomechanics. Chalm, Switzerland: Springer International Publishing AG.

Hoyt K, Hester FA, Bell RL, Lockhart ME, Robbin ML (2009) Accuracy of volumetric flow rate measurements: An in vitro study using modern ultrasound scanners. J Ultrasound Med 28:1511–1518.

Ikawa M, Karita K (2015) Relation between blood flow and tissue blood oxygenation in human fingertip skin. Microvasc Res 101:135–142.

Jacob M, Chappell D, Becker BF (2016) Regulation of blood flow and volume exchange across the microcirculation. Crit Care 20:319.

Johnson JM, Brengelmann GL, Hales JR, Vanhoutte PM, Wenger CB (1986) Regulation of the cutaneous circulation. Fed Proc 45:2841–2850.

Jones O (2017) TeachMeAnatomy.info. Available at: http://teachmeanatomy.info/upper-limb/vessels/arteries/; accessed May 16, 2018.

Kagaya A, Ohmori F, Okuyama S, Muraoka Y, Sato K (2010) Blood flow and arterial vessel diameter change during graded handgrip exercise in dominant and non-dominant forearms of tennis players. Adv Exp Med Biol 662:365–370.

Kammers MPM, Rose K, Haggard P (2011) Feeling numb: Temperature, but not thermal pain, modulates feeling of body ownership. Neuropsychologia 49:1316–1321.

Kammers MPM, Verhagen L, Dijkerman HC, Hogendoorn H, De Vignemont F, Schutter DJLG (2009) Is This Hand for Real? Attenuation of the Rubber Hand Illusion by Transcranial Magnetic Stimulation over the Inferior Parietal Lobule. J Cogn Neurosci 21:1311–1320.

Lane T, Yeh SL, Tseng P, Chang AY (2017) Timing disownership experiences in the rubber hand illusion. Cogn Res Princ Implic 2:4.

Lee J, Jirapatnakul AC, Reeves AP, Crowe WE, Sarelius IH (2009) Vessel diameter measurement from intravital microscopy. Ann Biomed Eng 37:913–926.

Li S, McDicken WN, Hoskins PR (1993) Blood vessel diameter measurement by ultrasound. Physiol Meas 14:291–297.

Lin GS, Spratt RS (1997) Hemodynamic imaging with pulsatility-index and resistive-index color Doppler US. Radiology 204:870–873.

Longo MR, Schüür F, Kammers MPM, Tsakiris M, Haggard P (2008) What is embodiment? A psychometric approach. Cognition 107:978–998.

Marasco PD, Kim K, Colgate JE, Peshkin MA, Kuiken TA (2011) Robotic touch shifts perception of embodiment to a prosthesis in targeted reinnervation amputees. Brain 134(Pt 3):747–758.

Maulik D (2005) Physical Principles of Doppler Ultrasonography. In: Maulik D (ed) Doppler Ultrasound in Obstetrics and Gynecology. Berlin, Heidelberg: Springer, pp. 9-17.

Moseley GL, Olthof N, Venema A, Don S, Wijers M, Gallace A, Spence C (2008) Psychologically induced cooling of a specific body part caused by the illusory ownership of an artificial counterpart. Proc Natl Acad Sci U S A 105:13169–13173.

Nelson TR, Pretorius DH (1988) The Doppler signal: Where does it come from and what does it mean? AJR Am J Roentgenol 151:439–447.

Ocklenburg S, Rüther N, Peterburs J, Pinnow M, Güntürkün O (2011) Laterality in the rubber hand illusion. Laterality 16:174–187.

Paton B, Hohwy J, Enticott PG (2012) The rubber hand illusion reveals proprioceptive and sensorimotor differences in autism spectrum disorders. J Autism Dev Disord 42:1870–1883.

Petersen LJ, Petersen JR, Talleruphuus U, Ladefoged SD, Mehlsen J, Jensen H (1997)

The pulsatility index and the resistive index in renal arteries. Associations with long-term progression in chronic renal failure. Nephrol Dial Transplant 12:1376–1380.

Pries AR, Reglin B, Secomb TW (2005) Remodeling of blood vessels: Responses of diameter and wall thickness to hemodynamic and metabolic stimuli. Hypertension 46:725–731.

Ramakonar H, Franz EA, Lind CRP (2011) The rubber hand illusion and its application to clinical neuroscience. J Clin Neurosci 18:1596–1601.

Ratcliffe N, Newport R (2017) The Effect of Visual, Spatial and Temporal Manipulations on Embodiment and Action. Front Hum Neurosci 11:227.

Rohde M, Di Luca M, Ernst MO (2011) The Rubber Hand Illusion: Feeling of ownership and proprioceptive drift do not go hand in hand. PLoS One 6:e21659.

Rohde M, Wold A, Karnath HO, Ernst MO (2013) The human touch: Skin temperature during the rubber hand illusion in manual and automated stroking procedures. PLoS One 8:e80688.

Rubin JM, Tuthill TA, Fowlkes JB (2001) Volume flow measurement using Doppler and grey-scale decorrelation. Ultrasound Med Biol 27:101–109.

Sivanandam S, Anburajan M, Venkatraman B, Menaka M, Sharath D (2012) Medical thermography: A diagnostic approach for type 2 diabetes based on non-contact infrared thermal imaging. Endocrine 42:343–351.

Smit M, Kooistra DI, van der Ham IJM, Dijkerman HC (2017) Laterality and body ownership: Effect of handedness on experience of the rubber hand illusion.

Laterality 22:703–724.

Sumpio BE (2000) Foot ulcers. N Engl J Med 343:787–793.

Sung CK, Lee KH, Kim SH (2017) Evaluation of factors influencing arterial Doppler waveforms in an in vitro flow phantom. Ultrasonography 36:39–52.

Tabrizchi R, Pugsley MK (2000) Methods of blood flow measurement in the arterial circulatory system. J Pharmacol Toxicol Methods 44:375–384.

Takayama S, Watanabe M, Kusuyama H, Nagase S, Seki T, Nakazawa T, Yaegashi N (2012) Evaluation of the effects of acupuncture on blood flow in humans with ultrasound color Doppler imaging. Evid Based Complement Alternat Med 2012:513638.

Tsakiris M (2010) My body in the brain: A neurocognitive model of body-ownership. Neuropsychologia 48:703–712.

Valenzuela Moguillansky C, O'Regan JK, Petitmengin C (2013) Exploring the subjective experience of the "rubber hand" illusion. Front Hum Neurosci 7:659.

van Netten JJ, van Baal JG, Liu C, van der Heijden F, Bus SA (2013) Infrared thermal imaging for automated detection of diabetic foot complications. J Diabetes Sci Technol 7:1122–1129.

Zierler BK, Kirkman TR, Kraiss LW, Reiss WG, Horn JR, Bauer LA, Clowes AW, Kohler TR (1992) Accuracy of duplex scanning for measurement of arterial volume flow. J Vasc Surg 16:520–526.